

2016-01-01

Controls On Carbonate Sedimentation And Sequence Stratigraphic Framework Of The Lower Permian (wolfcampian) Hueco Formation (upper-Middle And Gastropod Intervals), Robledo Shelf, Western Orogrande Basin, New Mexico

Matthew S. Harder

University of Texas at El Paso, mharder42@gmail.com

Follow this and additional works at: https://digitalcommons.utep.edu/open_etd



Part of the [Geology Commons](#), and the [Sedimentology Commons](#)

Recommended Citation

Harder, Matthew S., "Controls On Carbonate Sedimentation And Sequence Stratigraphic Framework Of The Lower Permian (wolfcampian) Hueco Formation (upper-Middle And Gastropod Intervals), Robledo Shelf, Western Orogrande Basin, New Mexico" (2016). *Open Access Theses & Dissertations*. 661.

https://digitalcommons.utep.edu/open_etd/661

This is brought to you for free and open access by DigitalCommons@UTEP. It has been accepted for inclusion in Open Access Theses & Dissertations by an authorized administrator of DigitalCommons@UTEP. For more information, please contact lweber@utep.edu.

CONTROLS ON CARBONATE SEDIMENTATION AND SEQUENCE
STRATIGRAPHIC FRAMEWORK OF THE LOWER PERMIAN
(WOLFCAMPIAN) HUECO FORMATION (UPPER-MIDDLE AND
GASTROPOD INTERVALS), ROBLEDO SHELF, WESTERN OROGRANDE
BASIN, NEW MEXICO

MATTHEW STEVEN HARDER

Master's Program in Geological Sciences

APPROVED :

Katherine A. Giles, Ph.D., Chair

Richard P. Langford, Ph.D.

Greg H. Mack, Ph.D.

Charles Ambler, Ph.D.

Dean of the Graduate School

Copyright ©

by

Matthew Steven Harder

2016

Dedication

This work is dedicated to all of my family and friends who supported my desire for science and enabled me to further my education.

CONTROLS ON LOWER PERMIAN (WOLFCAMPIAN) CARBONATE
SEDIMENTATION AND SEQUENCE STRATIGRAPHIC FRAMEWORK OF
THE HUECO FORMATION (UPPER-MIDDLE AND GASTROPOD
MEMBERS), ROBLEDO SHELF, WESTERN OROGRANDE BASIN, NEW
MEXICO

MATTHEW STEVEN HARDER, B.S.

THESIS

Presented to the Faculty of the Graduate School of

The University of Texas at El Paso

In Partial Fulfillment

of the Requirements

for the Degree of

MASTER OF SCIENCE

Geological Sciences

THE UNIVERSITY OF TEXAS AT EL PASO

August 2016

Acknowledgements

I would like to begin by thanking Dr. Katherine Giles for her undeniable expertise in sedimentology and stratigraphy, providing the necessary tools and support for myself to complete this project and develop into a research scientist and a professional geologist. I thank you dearly for the education you have provided me with and the avenues that are now open for my career. I would also like to acknowledge Dr. Greg Mack for being an exceptional teacher, geologist, and mentor, while we traversed across the peaks and valleys of the Doña Ana Mountains, measuring sections, collecting samples, and helping me become the geologist and person I am today. I feel incredibly lucky to have had this opportunity.

In addition I would like to thank Dr. Richard Langford, an exceptional geologist that sparked questions and expanded my curiosity towards all aspects of geology, science, and life through being exceptional educators. Also, this would not be possible without the help of all of the students I worked with and taught at both the University of Texas at El Paso and New Mexico State University. Special thanks also go out to Nila Matsler for providing unlimited logistical help over the past few years.

Abstract

On the western margin of the Pennsylvanian/Permian Orogrande Basin, two composite measured sections in the Lower Permian upper interval of the Middle Member of the Hueco Limestone were analyzed in regards to depositional environment, facies and sequence stratigraphy. This can elucidate where potential unconventional reservoirs can be found in the Wolfcamp Shale of the Permian Basin. Based on these analyses, 12 lithofacies were identified, including 9 carbonate lithofacies: 1) fenestral dolomudstone, 2) peloidal dolomudstone, 3) ostracode foraminifera packstone, 4) foraminifera peloidal grainstone, 5) skeletal intraclast grainstone, 6) phylloid algal peloidal grainstone, 7) echinoderm phylloid algal packstone, 8) echinoderm bivalve brachiopod packstone, and 9) *Tubiphytes* red algal packstone, and 3 siliciclastic lithofacies: 1) dull gray shale, 2) quartz siltstone, and 3) vertic calcisol. The carbonate lithofacies were organized into 4 depositional facies associations: 1) supratidal, 2) intertidal, 3) tidal channel, and 4) subtidal. Waltherian facies changes between these depositional facies associations indicates that the western margin of the Orogrande Basin was a shallow carbonate ramp with an incised valley located in the Doña Ana Mountains, creating a concentration of tidal channel, subtidal, and fluvial depositional facies in the area, this shows that fluvial systems in this area were funneled into the basin through topographic lows creating point sources for siliciclastics coming into the basin. In the Robledo Mountains, the Hueco Limestone experienced more restriction from the open ocean, creating a concentration of intertidal lagoons and supratidal flats with water chemistries that can vary greatly from normal marine seawater. Changes in the facies were controlled by changes in relative sealevel, driven by glacio-eustacy, as well as basin subsidence. The Gastropod interval experienced four fourth order sequences from base to top as part of one third order sequence. The upper interval of the Middle Member of

the Hueco Limestone experienced just one fourth order sequence, due to its having greater bathymetric relief. The sequence stratigraphic analysis shows that the upper interval of the Middle Member and the Gastropod interval of the Hueco Limestone correlate to each other, though the upper interval of the Middle Hueco experienced less depositional time.

Table of Contents

	Page
Acknowledgements.....	iv
Abstract.....	v
Table of Contents.....	vii
List of Figures.....	ix
Chapter 1: Introduction	1
1.1 Geologic Setting.....	2
1.2 The Orogrande Basin	4
1.3 Wolfcampian Stratigraphy.....	6
1.4 Previous Work.....	7
1.5 Methods	8
1.6 Formational Correlation.....	9
Chapter 2: Lithofacies Analysis	10
2.1 Lithofacies	10
2.1.1 Carbonate Supratidal Depositional Facies Association	10
2.1.2 Carbonate Intertidal Depositional Facies Association.....	15
2.1.3 Carbonate Tidal Channel Depositional Facies Association.....	21
2.1.4 Carbonate Subtidal Depositional Facies Association.....	26
2.1.5 Siliciclastic Terrestrial Depositional Facies Association.....	31
2.1.6 Siliciclastic Offshore Marine Depositional Facies Association.....	34
2.3 Depositional Profile Geometry.....	35
Chapter 3 Sequence Stratigraphy.....	38
3.1 Depositional Sequence Stratigraphy	38

3.2 Parasequence Types	39
3.3 Sequences	44
Chapter 4: Fischer Plot Analysis.....	49
Chapter 5: Controls on Lithofacies Distribution.....	52
5.1.1 Siliciclastics.....	52
5.1.2 Carbonates.....	54
5.2 Middle Wolfcampian Regression.....	55
Chapter 6: Conclusions.....	57
References.....	62
Vita.....	70

List of Figures

	Page
Figure 1: Paleogeographic Map of Area.....	2
Figure 2: Diagram of Orogrande Basin and Adjacent Uplifts.....	4
Table 1: Stratigraphy Chart of Hueco Limestone.....	6
Figure 3: Location of Outcrop Exposures and Measured Sections.....	8
Table 2: Lithofacies Table.....	11
Figure 4: Measured Section with Lithofacies.....	12
Figure 5: Photograph of Fenestral Dolomudstone Lithofacies.....	13
Figure 6: Photograph of Peloidal Dolomudstone Lithofacies.....	16
Figure 7: Photograph of Ostracode Foram Peloidal Packstone Lithofacies.....	19
Figure 8: Lagoon Types.....	20
Figure 9: Photograph of Foram Peloidal Grainstone Lithofacies.....	23
Figure 10: Photograph of Phylloid Algal Peloidal Grainstone Lithofacies.....	25
Figure 11: Photograph of Echinoderm, Phylloid Algal, Bivalve Packstone Lithofacies.....	25
Figure 12: Photograph of Echinoderm, Bivalve, Brachiopod Packstone Lithofacies.....	29
Figure 13: Photograph of Tubiphytes Red Algal Packstone Lithofacies.....	31
Figure 14: Photograph of Quartz Siltstone Lithofacies.....	32
Figure 15: Photograph of Vertic Calcisol Lithofacies.....	33
Figure 16: Photograph of Gray Shale Lithofacies.....	35
Figure 17: Depositional Profile.....	36
Figure 18: Parasequence Types.....	40
Figure 19: Measured Section with Sequence Stratigraphic Correlations.....	41
Figure 20: Measured Section with Correlations Facies.....	47

Figure 21: Fischer Plot.....	50
Figure 22: Paleoshoreline.....	51
Figure 23: Permian Eustatic Sea Level Curve.....	56

Chapter 1: Introduction:

This study focuses on depositional facies and stratigraphic studies of the upper-middle and gastropod intervals of the Hueco Limestone. The intervals are generally thought to be age correlative (Upper Wolfcamp), but lithologically different enough to warrant classification as separate lithologic members unlike the rest of the Hueco Limestone in the area (Seager et al., 2008). The correlatability and cause of the lithologic differences has not been determined. Using depositional sequence stratigraphy this study will test the hypothesis that the upper-middle and gastropod intervals of the Hueco Limestone are correlative, and that the cause of the lithologic differences is due to differences in depositional bathymetric relief between the two areas.

In recent years the West Texas Wolfcampian section of the Permian Basin has become one of the most prolific hydrocarbon plays in the United States due to advances in unconventional drilling techniques (Flumerfelt, 2015). This has increased the need to identify the controls on the spatial and temporal distribution of unconventional reservoir facies such as, organic-rich siltstone, within the Wolfcampian age section in order to better predict subsurface targets. The Orogrande Basin is adjacent to the Permian Basin and experienced a similar depositional and tectonic history, and contains well exposed correlative Wolfcampian strata, the Hueco Limestone. Utilizing petrographic and stratigraphic datasets collected from outcropping Hueco Limestone on the western margin of the Orogrande Basin, regional and local controls on sedimentation were determined in order to elucidate where potential unconventional reservoirs can be found in the subsurface and what their extent may be.

1.1 Geologic Setting

Located in southern New Mexico and West Texas the Permian and Orogrande basins are Upper Paleozoic depocenters that were generated by Ancestral Rocky Mountains tectonism (Fig. 1) (Kluth and Coney, 1981; Kues and Giles, 2004). During this period of time, collision between Laurentia and Gondwanaland formed the Ouachita-Marathon orogenic belt in Oklahoma and

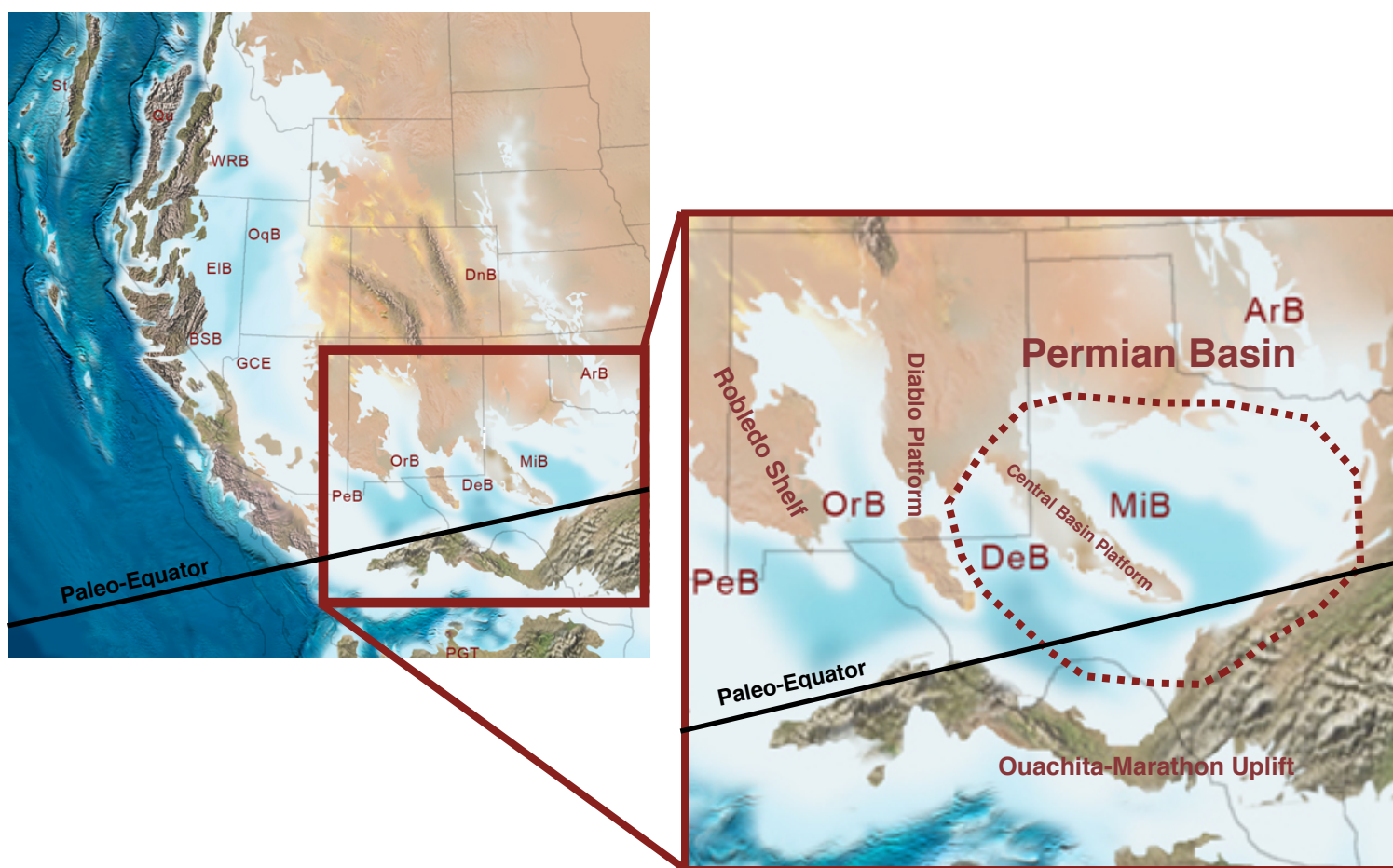


Figure 1: Early Permian paleogeographic map showing the Permian Basin and other basins within the southern part of the Ancestral Rocky Mountain Region in Texas and New Mexico (states outlined in gray). Individual basins labeled: PeB - Pedregosa Basin, OrB - Orogrande Basin, DeB - Delaware Basin, MiB - Midland Basin, ArB - Ardmore Basin modified from (modified from Blakey 1980)

Texas, and provided the structural setting for the development of the Ancestral Rocky Mountains foreland orogenic belt (Graham et al., 1975; Kluth and Coney, 1981; Ross and Ross, 1986; Algeo, 1992) (Fig. 1). Most of the basins associated with the Ancestral Rocky Mountains uplifts were in tropical to sub-tropical latitudes, with carbonate production centered around the southern and western margins of Laurentia (Fig. 1).

The late Paleozoic is known for its distinctive global-scale sedimentary cycles driven by glacio-eustatic sea-level fluctuations (Ross and Ross, 1988). Strata of this age were deposited as part of the Absaroka Megasequence driven by the large-scale continental glaciation of Gondwana, leading to an icehouse climate (Sloss, 1963; Wanless and Cannon, 1966; Heckel, 1977; Vail et al., 1987). Late Paleozoic glacio-eustatic sealevel changes were high frequency (<100,000 years) and high amplitude (>60m) (Soreghan and Giles, 1999; Olszewski and Patzkowsky 2003).

During the Paleozoic, planktonic sources of carbonate sediment had not yet evolved carbonate sedimentation thus all carbonate sediments in deep basinal settings were derived from downslope transport from the shallow shelf into the basinal setting because (Gartner, 1977). Therefore, Wolfcampian-age basinal carbonate sedimentation patterns and depocenters can be predicted by studying the shelf equivalent facies, which were the source (Mazzullo, 1989). Mechanisms for moving carbonate sediment from the shelf to the basin are primarily different types of gravity flows (Miller and Heller, 2006; including turbidity flows, debris flows, and grain flows (Pujalte et al., 1993).

1.2 The Orogrande Basin

The subsurface Delaware and Midland basins collectively form the Permian Basin (Fig. 1) and are partially separated by the Central Basin Platform. The Diablo Platform forms the eastern margin of the Orogrande Basin and separates it from the Permian Basin (Fig. 2).

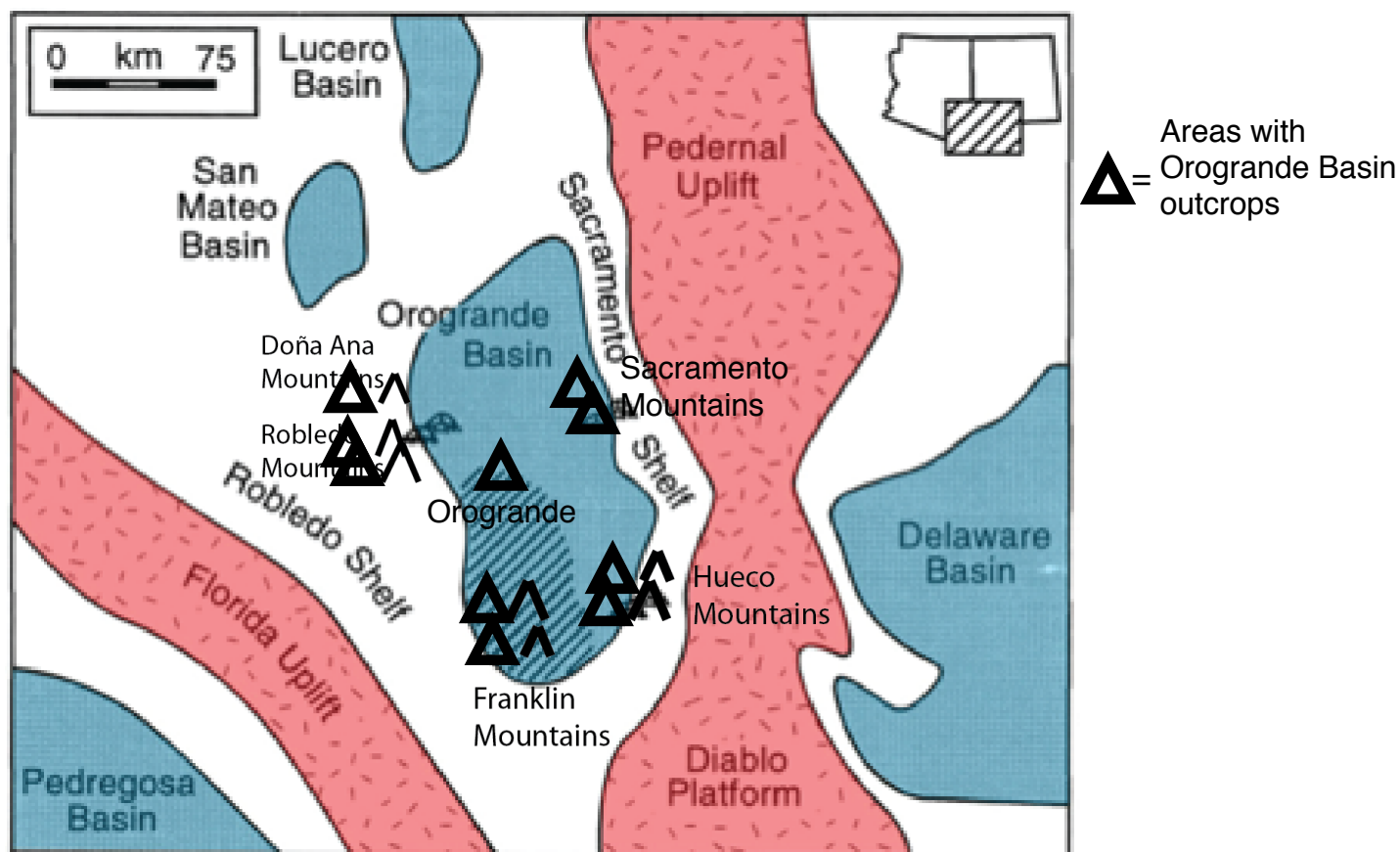


Figure 2: Paleogeographic map showing the locations of Permian Ancestral Rocky Mountain uplifts (in red) and basins (in blue) of southern new Mexico and Arizona as well as modern mountain ranges containing outcrops of the Hueco Limestone in the Orogrande Basin (modified from Kues and Giles, 2004).

The Orogrande Basin subsided from Pennsylvanian to mid-Permian time (Kues and Giles, 2004). During the late Mississippian to early Pennsylvanian, initial uplift began of the adjacent Pedernal landmass and Diablo Platform (Fig. 2). Carbonate deposition began on the

eastern margin of the Orogrande Basin during the early Pennsylvanian (early Atokan), mainly as open marine carbonate sedimentation with local large phylloid algal buildups (Connally and Stanton, 1983).

During the Atokan major marine transgression spread marine environments from the Orogrande Basin into northwest New Mexico (Kues and Giles, 2004). Marine carbonate deposition continued around the entire basin margin on low angle and distally-steepened ramps while the center of the basin was dominated by shales and thin carbonate mudstones (Jordan, 1975; Wilson and Jordan, 1975; Mack and James, 1986)

The Early Permian (Wolfcampian) in North America marks a significant climatic shift from the Pennsylvanian icehouse climate dominated by glacio-eustatic sea-level fluctuations to a more temperate, drier climate (Ross and Ross, 1990; Mack, 2003). This change continued into the Leonardian leading to a more arid climate with, lower magnitude sealevel fluctuations (Kessler, et al., 2001; Mack and James, 1986). Lower Permian strata record an important transition in Earth's climate history, which is preserved in the Hueco Limestone.

Wolfcampian strata in the Orogrande Basin were deposited during a second-order marine transgression induced by a glacio-eustatic sea-level rise that followed the major sea-level low stand at the Pennsylvanian-Permian boundary (Kues and Giles, 2004). Marine strata associated with this transgression overlapped and overlapped highlands that were being eroded during the waning stages of Ancestral Rocky Mountain uplift (Kottlowski, 1963). Exposures of these marine sequences (Hueco Limestone), are found in the Hueco, Franklin, Organ, San Andreas, Robledo, and Doña Ana mountains of west Texas and southern New Mexico (King, 1934; Williams, 1963; Kottlowski and Seager, 1988). To the northeast in the Sacramento Mountains,

the Hueco Limestone contains strata that display rapid lateral facies changes from mudstones to sandstones and conglomerates, and local shelf-margin phylloid algal buildups (Wilson, 1975).

1.3 Wolfcampian Stratigraphy

Previous mapping and biostratigraphic studies of the Hueco Limestone in the Robledo and Doña Ana mountains used the older informal nomenclature of lower, middle, and upper members (Fig. 3) (Seager et al., 2008), including the Abo Tongue, correlative to the Abo Formation to the north and the Red Mountain Shale to the east (Kottlowski, 1960, 1963; Jordan

Table 1: Correlation diagram showing Wolfcampian stratigraphy of the Robledo and Doña Ana mountains with the stratigraphic units of this study highlighted in blue. International stage ages from Cohen et al. (2013).

Lower Permian	Age	N.A. Stage	Robledo Mountains (Mack et al., 2013)		Doña Ana Mountains (Seager et al., 2008)		Robledo Mountains (Lucas et al., 1998)	
	International Stage							
	279.3 Ma	Wolfcampian	upper Hueco member		upper Hueco member		Apache Dam Formation	
	Artinskian							
	290.1 Ma		Abo Tongue		Abo Tongue		Robledo Mountains Formation	
	Sakmarian		middle Hueco member	upper interval	middle Hueco member	gastropod interval	Community Pit Formation	
				lower interval		lower interval		
lower Hueco member			upper interval	lower Hueco member				
		lower interval						
295.5 Ma					Shalem Colony Formation			
Asselian								
298.9 Ma								

1971; Mack and James, 1986). Lucas et al. (1998) applied formal names to the members of the Hueco Limestone in the Robledo Mountains, which are in ascending order: Shalem Colony Formation, Community Pit Formation, Robledo Mountains Formation, and Apache Dam Formation. These formations are difficult to recognize and correlate to the Doña Ana Mountains stratigraphy. As a result this study will use the informal subdivisions made by Kottlowski (1960) and subdivisions made by Mack et al. (2013), which are generally correlatable between the two locales.

1.4 Previous Work

Numerous researchers have studied the Hueco Limestone in order to address a variety of different problems. The early work was mainly focused on characterizing and defining Wolfcampian stratigraphy in the Orogrande Basin. King et al. (1945), Kottlowski et al. (1956), Williams (1963), Jordan (1971), Seager (1981), and others used regional mapping and widely spaced measured stratigraphic sections to construct the general stratigraphic framework of the Wolfcampian strata in the Orogrande Basin. These studies were focused on regional lithostratigraphic and biostratigraphic correlation, not detailed facies and depositional environment interpretation, which will be the focus of this study. One of the first detailed lithostratigraphic studies was completed by Jordan (1975) in order to correlate Wolfcampian stratigraphy on the eastern Sacramento Shelf (Laborcita Formation) on the eastern edge of the Orogrande Basin to the Hueco Limestone, on the western edge. No detailed petrographic analysis, depositional environments, or sequence stratigraphic analysis has been completed on the upper-middle and gastropod interval of the Hueco Limestone.

1.5 Methods

Three composite stratigraphic sections, two in the Robledo Mountains and one in the Doña Ana Mountains (Fig. 4), were measured using a 1.5-meter Jacobs staff, a Brunton compass,

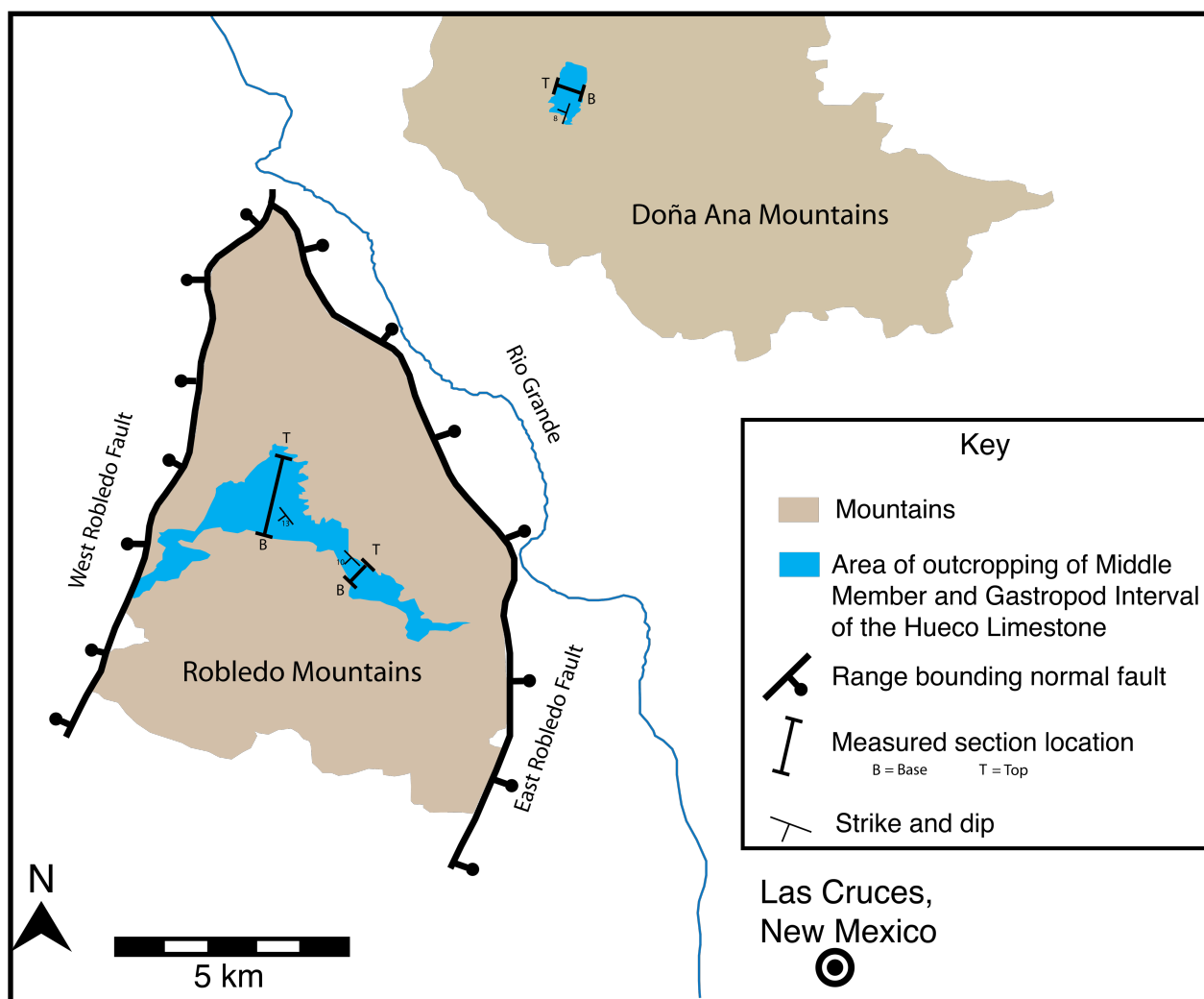


Figure 3: Map of the Middle Hueco Limestone outcrops in the Robledo Mountains and gastropod interval outcrops in the Doña Ana Mountains and locations of measured stratigraphic sections. (Modified from Seager et al., 2008.)

and GPS coordinates, taken with a handheld GPS. Fifty-four hand samples were collected from each major change in lithology and petrographic thin sections prepared by Petrographic Services

Company from selected hand samples. The samples were stained with alizarin red stain for calcite and potassium ferricyanide stain for iron content in carbonate minerals. Petrographic samples were analyzed using a Leica petrographic microscope to augment field description of lithologic characteristics. The lithofacies were interpreted and placed into a depositional facies model in order to interpret sequence stratigraphic framework. A Fisher Plot analysis was also done on the two composite sections in order to track accommodation trends as described by Read and Goldhammer, (1988). The sequence stratigraphic framework and Fisher Plot analysis provided high resolution methods of correlation between the Robledo and Doña Ana mountain Wolfcampian sections.

1.6 Formational Correlation

The base of the Abo Tongue member of the Hueco Limestone was utilized to correlate between the Robledo and Doña Ana Mountains sections (Seager, 2008). The base of the gastropod interval of the Middle Member of the Hueco Limestone, which is only found in the Doña Ana Mountains, and the base of the upper interval of the Middle Member of the Hueco Limestone as defined by Mack et al. (2013) only found in the Robledo Mountains are only generally correlatable. The sections were measured from the top of the lower interval of the Middle Member to the base of the Abo Tongue.

Chapter 2 Results

2.1 Lithofacies and Depositional Facies Associations

Outcrop and hand sample observation of lithologic and sedimentological features along with petrographic analysis was used to determine the lithofacies observed in the gastropod interval and upper interval of the Middle Member of the Hueco Limestone exposed in the Robledo and Doña Ana mountains (see Figure 5). Twelve distinct lithofacies were identified including 9 carbonate facies, and 3 siliciclastic facies (see Table 1). The carbonate lithofacies are: 1) fenestral dolomudstone, 2) peloidal dolomudstone, 3) ostracode foraminifera peloidal packstone, 4) foraminifera peloidal grainstone, 5) skeletal intraclast grainstone, 6) phylloid algal peloidal grainstone, 7) echinoderm phylloid algal bivalve packstone, 8) echinoderm bivalve brachiopod packstone, and 9) *Tubiphytes* red algal packstone. The siliciclastic lithofacies are: 1) quartz siltstone, 2) vertic calcisol, and 3) gray shale (Fig. 5). The attributes of these lithofacies are summarized in Table 1 and their stratigraphic distribution are on the measured sections shown in Figure 5. The lithofacies were grouped into 4 carbonate depositional facies associations, which are listed below according to their relative position on a marine shoreline to basin depositional profile: 1) supratidal carbonate, 2) intertidal carbonate, 3) tidal channel, and 4) subtidal carbonate. The siliciclastic lithofacies were grouped into two depositional facies associations: 1) terrestrial, and 2) offshore marine (Table 1).

2.1.1 Carbonate Supratidal Depositional Facies Association

This depositional facies association contains the fenestral dolomudstone lithofacies. Supratidal facies were deposited in a near shoreline environment, in protected areas from high

Table 2. Table listing the characteristics of each lithofacies and depositional environment interpretations.

	Lithofacies	Depositional Facies Association	Color		Bed		Grain Types a=abundant r=rare		Sed Structures	Diagenetic Features a=abundant r=rare	
			Fresh	Weathered	Thickness (cm)	Style	Skeletal	Non-skeletal		Cement	Other
Carbonate	Fenestral Dolomudstone	Supratidal	Light gray, Tan	Yellow, Tan	10 to 20	Slightly Undulose		Peloids (a)	Stromatolites Wavy laminations	Dolomite (r) Calcite (a)	Calcite pseudomorphs after gypsum Dolomitization
	Peloidal dolomudstone	Intertidal Lagoon	Light gray, Tan	Yellow, Tan	20 to 100	Slightly Undulose		Peloids (a)	Bioturbation	Silica (r) Dolomite (a) Calcite (r)	Dolomitization (a) Silicification (r)
	Ostracode foram peloidal packstone	Intertidal Lagoon	Dark gray	Medium gray	50 to 500	Slightly Undulose	Forams (a) ostracodes (a)	Peloids (a) Intraclasts (r)		Calcite (a)	Silicification (r)
	Foram peloidal grainstone	Tidal Channel	Light gray	Light gray	20 to 40	Planar	Forams (a) gastropods (r)	Peloids (a) Intraclasts (a)		Calcite (a)	Silicification (r)
	Skeletal Intraclast grainstone	Tidal Channel	Light gray	Medium gray	20 to 40	Planar	Crinoids (r) ostracodes (r) gastropods (r) bivalves (r) bryozoans (r)	Intraclasts (a)	Bi-directional current Crossbeds Ripples	Calcite (a)	Silicification (r)
	Phylloid Algal Peloidal Grainstone	Tidal Channel	Light gray	Medium gray	20	Planar	Phylloid algae (a)	Peloids (a)	Mud cracks	Calcite (a) Silica (r)	Silicification (r)
	Echinoderm phylloid algal bivalve packstone	Subtidal	Dark gray	Dark gray	30 to 500	Undulose	Phylloid algae (a) echinoderms (a) bivalves (a)	Peloids (r)	Burrowed		Silicification (r)
	Echinoderm Bivalve Brachiopod Packstone	Subtidal	Light gray	Light gray	40 to 500	Undulose	Phylloid algae (r) brachiopods (a) bivalve (a)		Bioturbation		Silicification (r)
	Tubiphytes Red Algal Packstone	Subtidal	Medium Gray	Medium Gray	30	Undulose	Tubiphytes (a) Red algae (a) Bryozoans (r)				Chert nodules (a)
Siliciclastic	Quartz siltstone	Terrestrial Fluvial	Tan	Tan	20 to 250	Undulose		Quartz silt (a)	Assymetrical ripples Lateral accretion sets		
	Vertic calcisol	Terrestrial Soil	Dull gray	Dull gray	30	Planar					Calcite nodules (a)
	Gray Shale	Offshore Marine	Dull gray	Dull gray	10 to 500	Planar			Silt Laminae		

wave energy. These areas were sub-aerially exposed for long periods of time with periodic inundation during spring tide events or storms. This environment is characterized by mineralization related to hyper saline and brackish water conditions such as displacive gypsum, similar to the arid sabkha environment documented along the Trucial Coast in the Middle East today (Shinn, 1983).

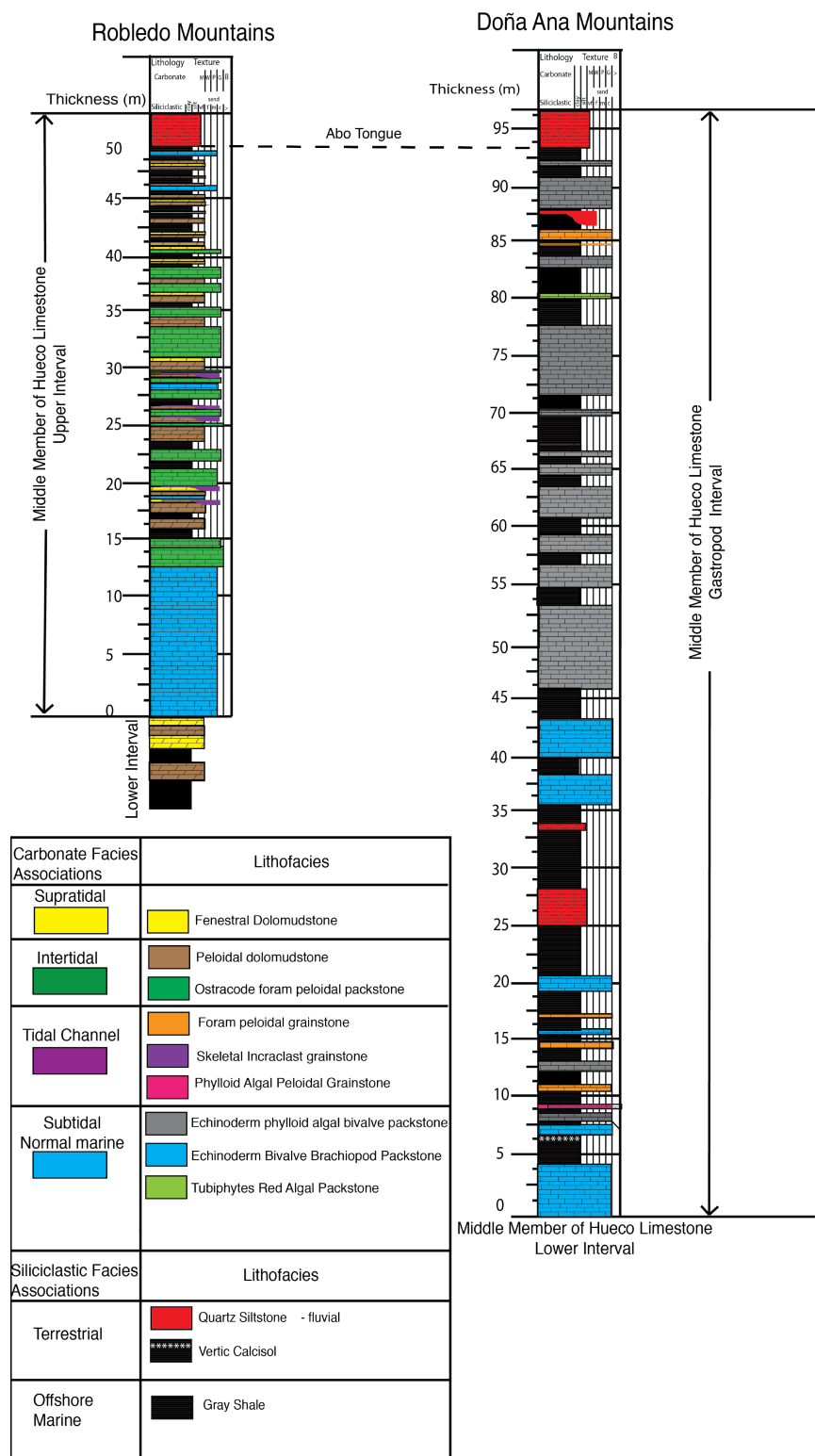


Figure 4. Measured sections from the Robledo and Doña Ana mountains with each lithofacies shown and the formational correlation with the overlying Abo Tongue.

Fenestral Dolomudstone Lithofacies

Fenestral dolomudstone is confined to exposures in the Robledo Mountains. Outcrops form both laterally continuous yellow and tan ledges or poorly exposed recessive slopes. Weathered outcrops range in color from yellow and tan with fresh surfaces usually appearing light gray or tan. Beds of this facies are thin ranging from 10 to 20 cm and have slightly undulose bedding. Many beds contain irregular wavy laminations associated with stromatolitic cyanobacterial mats. Stromatolites are common within this lithofacies and occur as both digitate and laminated forms. One bed contained pebble-sized charcoal.

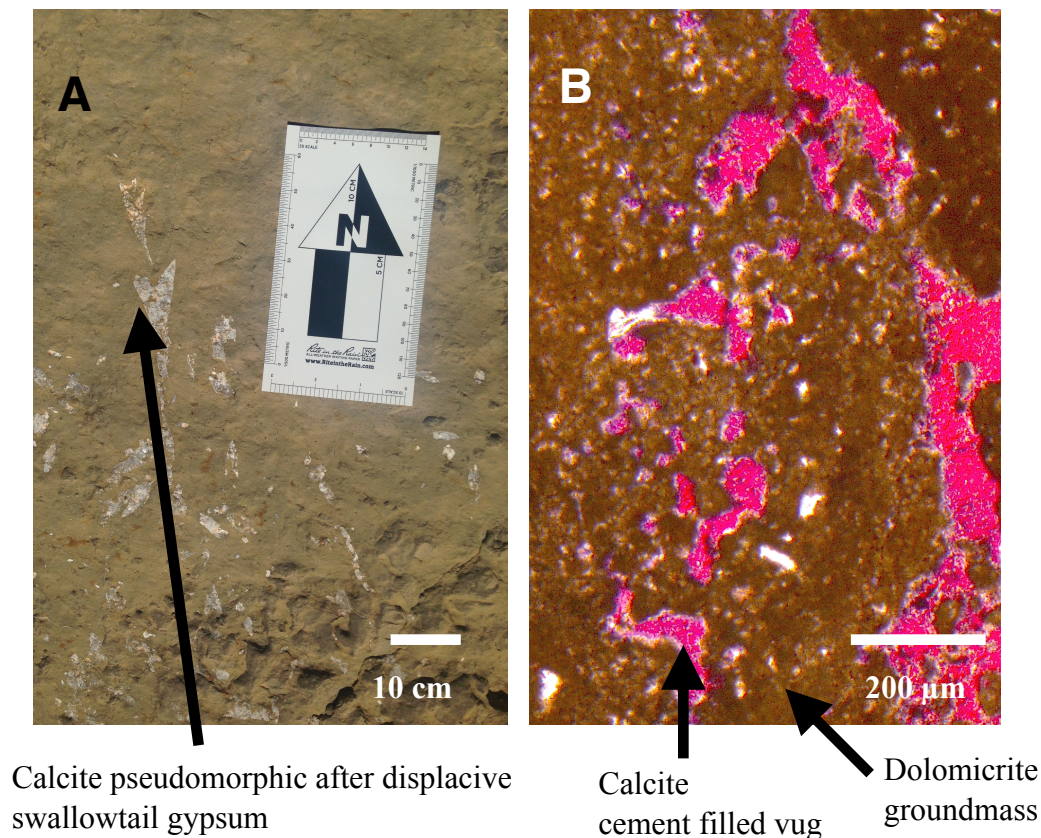


Figure 5. A. Photographs of the fenestral dolomudstone lithofacies: A) Outcrop photograph showing calcite pseudomorphs after displacive swallow tail gypsum B) Thin section photomicrograph of calcite-filled fenestral voids in peloidal dolomicrite groundmass.

The most distinguishing characteristic of this lithofacies is the dense microcrystalline dolomite and heavily micritized grains (Fig. 6). Non-fabric selective dolomitization is common in these beds. Dolomite and calcite cement is common and is typically found filling fenestral vugs. Calcite crystals is also common filling fenestral vugs and inter particle porosity with a druzy mosaic geometry. Calcite pseudomorphs after swallowtail gypsum are visible on outcrop.

Depositional Environment Interpretation

Three key attributes were considered when making environmental interpretations for fenestral dolomudstones: 1) pervasive dolomitization, 2) inter-laminated stromatolites, and 3) fenestral vugs within the heavily laminated intervals. *In-situ* dolomitization has been recognized on modern carbonate tidal flats, in the Netherlands Antilles (Wells, 1962), Bahamas (Deffeyes et al. 1965) and Persian Gulf (Illing et al. 1965 and Shinn et al., 1965). All of these studies confirm that dolomite can form in the supratidal zone on tidal flats as sea water is brought to the surface by capillary action or from storm induced flooding. Evaporation leaves highly concentrated brines that facilitate dolomite precipitation. Illing et al. (1965) documented a similar facies association in the Bahamas with dolomitic muds with stromatolitic cyanobacterial laminae underlying the upper most supratidal deposits, with very fine-grained peloidal muds sitting below the algal laminations. A similar relationship was observed in the Robledo Mountains.

Stromatolites are another common feature along carbonate coastlines across the world and throughout the geologic record. These thinly laminated mats would have grown within the supratidal and high intertidal environments (Shinn, 1983). Fenestral vugs are common throughout intervals with cyanobacterial laminations and are often filled with calcite cement or local quartz cements. Fenestral vugs form from the shrinkage of sediment surrounding gas

bubbles within algal mats as the gas bubbles escape to the air and represent reliable indicators of supratidal environments when found in muddy rocks (Fischer, 1964; Tebbutt, 1965; Shinn, 1983). In the Robledo Mountains, fenestral vugs are commonly inter-laminated between thin cyanobacterial laminations. Based on these factors, fenestral dolomudstones found in the middle Hueco member are considered to have developed on a supratidal flat similar to a modern day sabkha environment. Pervasive dolomitization, the presence of calcite pseudomorphs after gypsum suggest these environments were very arid as described by Shinn (1983).

2.1.2 Carbonate Intertidal Depositional Facies Association

Lithofacies within this depositional setting are: peloidal dolomudstone and ostracode foram wackestone to packstone. These lithofacies are found in a narrow zone parallel to the paleoshoreline and mark a distinct transition from supratidal facies that are often sub-aerially exposed, to the shallow marine subtidal zone that are not sub-aerially exposed for long periods of time. These rocks show evidence of semi-restricted environments with low current energy. Additionally, these facies form a facies mosaic with their relative position to each other dependent on local paleogeographic and/or bathymetric relief. The exact characteristics that describe how and where these rocks formed during the early Wolfcampian are described below.

Peloidal Dolomudstone Lithofacies

At outcrop scale, peloidal dolomudstone beds have a similar appearance to supratidal fenestral dolomudstone based on their color and composition, but the peloidal dolomudstone lacks laminations and has thicker beds. Outcrops form laterally continuous yellow, tan, and gray ledges. Most outcrops are thin to medium bedded, ranging from 20 to 100 cm, whereas fenestral dolomudstone beds are thin bedded. The peloidal dolomudstone facies contains more non-skeletal grains than the fenestral dolomudstone lithofacies. The most abundant consist of pellets and peloids.

The matrix consists of microcrystalline calcite and dolomicrite. Dolomite crystals are very small (<500 microns) (Fig. 7) and probably formed by recrystallizing microcrystalline

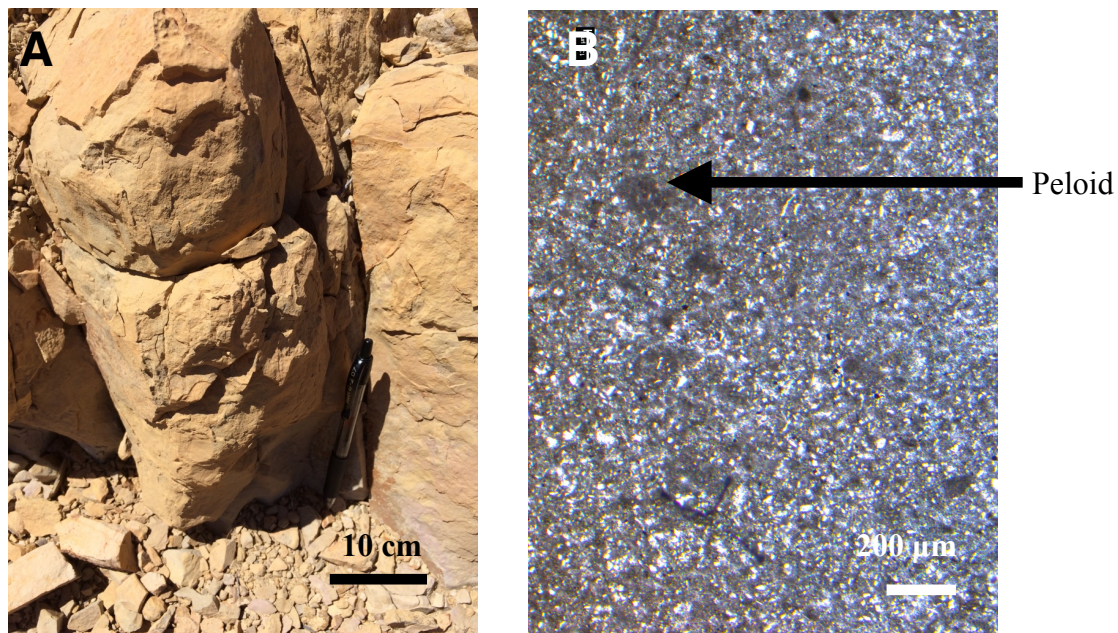


Figure 6. Peloidal dolomudstone lithofacies A) Outcrop photograph of bioturbated thin-medium beds B). Thin section photomicrograph of peloidal dolomudstone.

calcite crystals. Dolomitization appears to be non-fabric selective as it has altered both the matrix and non-skeletal grains to the same degree. However, the rims of the grains can be identified by the darker, finer-grained dolomite crystals that compose them. Silica cement is rare but calcite cements are abundant in small vugs, fractures, and interparticle porosity as calcite cement.

Depositional Environment Interpretations

Based on the characteristics described above, the peloidal dolomudstone appear very similar to fenestral dolomudstones but lack key features, such as fenestral fabric, laminations, and calcite pseudomorphs after swallowtail gypsum, observed in the fenestrate dolomudstones. Unlike fenestral dolomudstones, these dolomudstones lack laminations, which suggest extensive bioturbation, similar to Shinn (1983) documented on the Trucial Coast. The abundance of peloids are an indication of micritization of grains by endolithic algae (Bathurst, 1975). Peloid-rich environments have been documented in lagoonal sediments of the Trucial Coast (Kendall and Skipwith 1969). Environments that experience periodic hyper-saline conditions from a decrease in water circulation from sea-level changes or development of a barrier or shoal have potential to form conditions that would allow for dolomite precipitation at the sediment-water interface (Enos, 1983). These conditions would lead to a restricted faunal diversity, such as observed in the middle Hueco dolomudstones. The fine-grained texture suggests deposition in a lower energy regime that would allow finer-grained sediment to slowly settle out of the water column.

Enos (1983) identifies restricted shelfal lagoons and bays based on the style of shoaling upward cycles where basal muddy carbonates with low diversity faunas are overlain by

supratidal fenestral dolomudstones or other adjacent intertidal facies. Additionally, the muddy low energy restricted environments may contain facies mosaics of random transitions related to minor sea-level changes in shallow environments that create substantial changes in depositional environments (Laporte, 1967; Enos, 1983). Thin dolomudstone beds observed in the upper interval of the middle Hueco member are always interbedded with supratidal and other intertidal deposits (foram ostracode packstone and fenestral dolomudstone). Based on this relationship, along with the low faunal diversity, abundant micritized non-skeletal grains, and dolomitization, this lithofacies is interpreted as a restricted lagoon environment that led to very saline to hyper saline water chemistries and deposition of massive peloidal dolomudstone.

Ostracode Foram Peloidal Packstone Lithofacies

Non-fusulinid foraminifera are abundant in many different lithofacies across the Robledo Shelf and Orogrande Basin but this lithofacies has abundant ostracodes in addition that comprise over 30% of rock-forming grains. Outcrop exposures are medium gray in color on weathered surface and dark gray on fresh surfaces. Bed thickness is highly variable from thin to massive (0.5 to 5 meters thick).

Forams and ostracodes are the most abundant rock-forming grains in this lithofacies.. Locally rare fragments of crinoids, bryozoans, and bivalves are present. Peloids are common and intraclasts are present rarely. The matrix is primarily composed of dense microcrystalline calcite, which gives hand samples and thin sections a dark gray appearance (Fig. 8). Calcite cement is common and usually forms equant blocky crystals filling voids or small fractures but most commonly occurs filling intraparticle porosity.

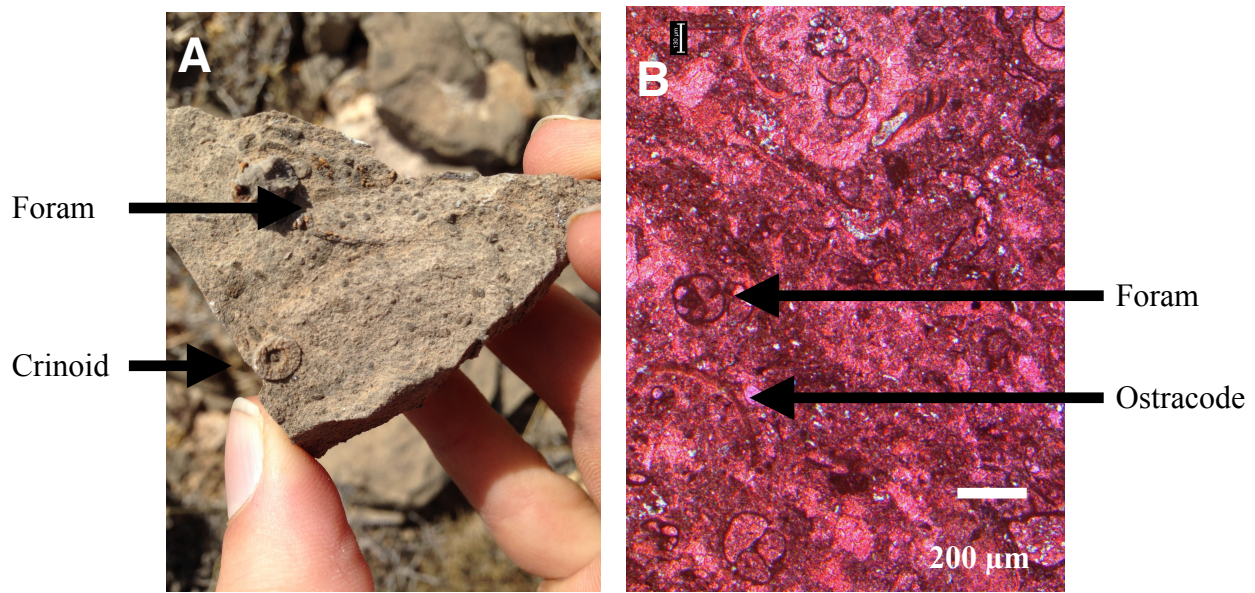


Figure 7. Photographs of ostracode foram peloidal packstone lithofacies. A) Photograph in hand sample with visible forams and crinoids. B) Thin section photomicrograph showing abundant forams.

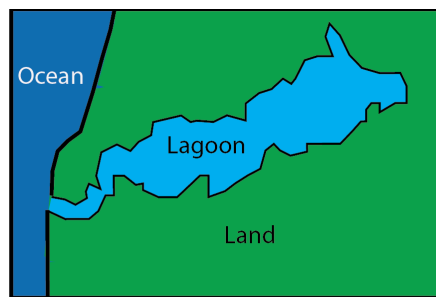
Depositional Environment Interpretation

Two key criteria listed above suggest that deposition of this lithofacies occurred in a low energy restricted lagoon or bay, where some type of outboard barrier dissipated wave energy before it could enter the lagoon. However, this lagoon would be much less restricted than the environment that produced the peloidal dolomudstone lithofacies as suggested by the the lack of dolomitization and greater faunal diversity. Enos (1983) also states that slow water circulation would result in depleted nutrients or abnormal salinities that would also inhibit faunal diversity, such as a lack of phylloid algae and/or brachiopods.

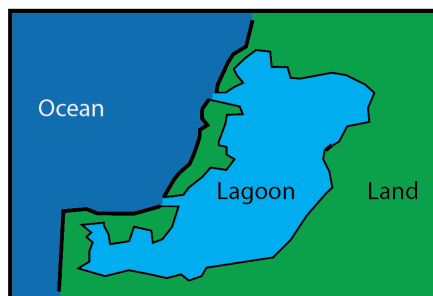
Enos (1983) describes semi-restricted, compartmentalized lagoons along the coast of Florida and along the northern coast of Cuba that contain rapid lateral and vertical facies transitions creating facies mosaics. Kjerfve (1986) classified coastal lagoons into three different

types based on the access to water circulation, river input, wind stress, tides, and precipitation of evaporites. These three types of lagoons are: 1) choked, which are characterized by a narrow entrance channel or at times are completely cut-off from the open ocean, 2) restricted, which are an intermediary between choked and leaky lagoons, and 3) leaky, which are connected to the open ocean by a series entrance channels (Fig. 9). Copeland (1967) and Moore and Slinn (1984) documented that in arid and semi-arid regions, choked lagoons often become hypersaline, similar

1. Choked



2. Restricted



3. Leaky



Figure 8. Three types of coastal lagoons. Modified from Kjerfve (1986): 1. Choked, 2. Restricted, 3. Leaky.

to the peloidal dolomudstone environment. Kjerfve (1986), documented restricted lagoons with brackish to oceanic salinities, similar to the ostracode foram peloidal packstone facies, and leaky lagoons with oceanic salinities and strong tidal currents.

In the gastropod interval and middle Hueco, ostracode foram packstones and wackestones contain an abundance of microcrystalline calcite mud, suggesting lower wave and tidal energy, allowing for deposition of fine-grained carbonate mud. Higher wave and tidal energy would have winnowed the mud out of the area, leaving only skeletal debris. Enos (1983) and Kjerfve (1994) both describe wind influences in modern day coastal lagoons in the Bahamas and on the Pacific coast of Mexico. This relationship suggests that ostracode foram peloidal packstone lithofacies represents a semi-restricted transitional environment between the supratidal and subtidal depositional environments.

2.1.3 Carbonate Tidal Channel Depositional Facies Association

This lithofacies association is dominated by high-energy grainstone facies including: foram peloidal grainstone, skeletal intraclast grainstone, and phylloid algal grainstone. Tidal channel deposits form basinward of the paleoshoreline in both the intertidal and shallow subtidal setting above fair-weather wave base. These facies have both an intertidal portion that is regularly subaerially exposed and a subtidal portion that is rarely subaerially exposed unless there is a significant spring tide or change in sea-level related to major eustatic events. This facies association is characterized by higher tidal current energy environments. No ooids were found in these facies indicating very little wave energy. The exact characteristics that describe how and where these rocks formed during the early Wolfcampian are described below.

Foram Peloidal Grainstone Lithofacies

The foram peloidal grainstone is only found in the Doña Ana Mountains near the top and the base of the section. The beds are laterally continuous and thin ranging in thickness from 20 to 40 cm and beds are generally planar to slightly undulose. This facies is light gray in both outcrop and on weathered surface.

Grains are dominated by peloids with some foraminifera fragments and intraclasts (Fig. 10) including fragments of shells as well as rare gastropod shells. The cement is made up of a blocky, equant calcite cement with larger calcite crystals filling in voids.

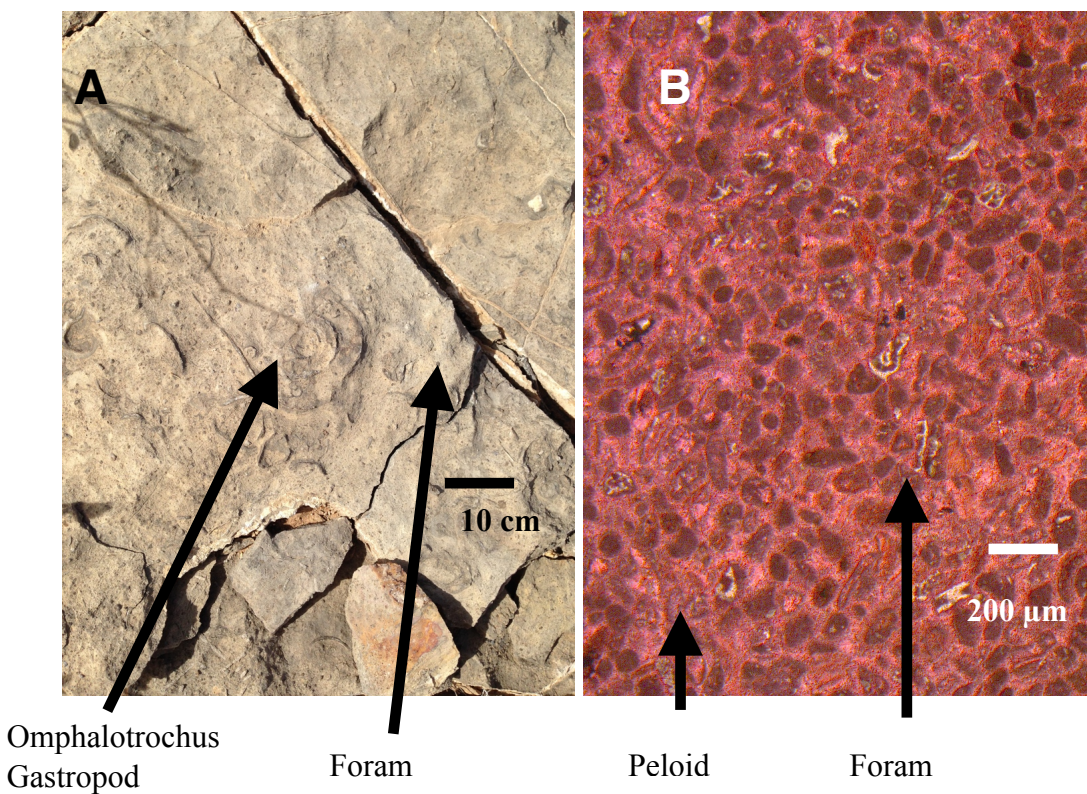


Figure 9. Photographs of the foram peloidal grainstone facies. A) Photograph of outcrop with larger omphalotrochus gastropod B) Photomicrograph displaying abundant peloids, forams, and intraclasts

Depositional Environment Interpretation

The key characteristics of this lithofacies that allow for identification of the depositional environment are the lack of carbonate mud, and the fine sand to silt sized grains and limited grain types. Both characteristics indicate that this was a high energy environment to sort grain size and winnow out finer-grained material. The restricted marine fossil assemblage indicates that the current energy reworking grains dominantly from the intertidal, restricted marine environment, which indicates that these were ebb tide dominated. Finally the thinness of the bed indicates that this lithofacies was deposited with little accommodation space, which suggests an environment that is close to the paleoshoreline in the high intertidal.

Skeletal Intraclast Grainstone Lithofacies

Skeletal intraclast grainstone beds range in thickness from 0.3 to 0.5 m, only in the Robledo Mountains. The laterally discontinuous beds have horizontal tops and erosive, convex-downward bases. The intraclast, grainstones truncate fenestral dolomudstone, peloidal dolomudstone, and foram packstone and grainstone lithofacies. The most common grains are intraclasts, which are composed of limestone and dolomudstone, the latter displaying textures similar to those of the fenestral dolomudstone and peloidal dolomudstone lithofacies. Fossil fragments, or skeletal clasts, are also common and include ostracodes, bivalves, gastropods, brachiopods, forams, echinoid spines, echinoderm columnals, and bryozoans. Bidirectional trough and planar crossbeds in sets 10 cm thick exist in most of the beds, as well as ripple cross-laminae.

Depositional Environment Interpretation

The skeletal intraclast grainstones were deposited in higher current energy tidal channels, based on basal erosional truncation, channel morphology, abundant skeletal and intraclasts, and bipolar cross- beds. The channels truncate supratidal and intertidal lithofacies, they probably traversed the supratidal, intertidal, and shallow subtidal zones, similar to tidal channels documented along the Trucial Coast (Kendall and Skipwith 1969; Evans et al. 1969; Bathurst 1975). Most of the fossils were disarticulated and broken during transport. The bipolar character of the cross-beds suggests that ebb and flood tides were of similar strength, which is consistent with the combination of limestone intraclasts that probably were derived from a seaward direction and dolomudstone intraclasts derived from the lagoon and intertidal-supratidal flat. The presence of dolomudstone intraclasts in the tidal channels also supports the idea of early dolomitization of supratidal, intertidal, and lagoonal dolomudstone. Mack et al. (2013) documented tidal channels in the lower interval of the Middle Member of the Hueco Limestone which were lateral equivalents of fenestral dolomudstone and peloidal dolomudstone lithofacies.

Phylloid Algal Peloidal Grainstone Lithofacies

The phylloid algae peloidal grainstone facies is only found in one bed, in the Doña Ana Mountains section. The bed was thin, (20 cm) and bedding was planar, but had mud cracks on top. On outcrop the facies was medium gray in color on the weathered surfaces and light gray on fresh surfaces. Grains types include large irregularly shaped peloids and phylloid algal grains that have been heavily recrystallized, and rare echinoderm debris. The cement is equant calcite

cement filling voids in between grains (Fig. 11). The phylloid algal grains have undergone recrystallization and are ferroan calcite or have been dissolved and filled with ferroan calcite cement. The peloids have undergone some silicification and isolated vugs in this lithofacies are filled with quartz cement.

Depositional Environment Interpretations

The key characteristics of this lithofacies that allow for identification of this depositional environment are the lack of carbonate mud and the fine sand carbonate. Both characteristics indicate that this was a high enough energy environment to winnow out finer-grained material. The larger average grain size indicates that tidal energy was higher in this lithofacies than the

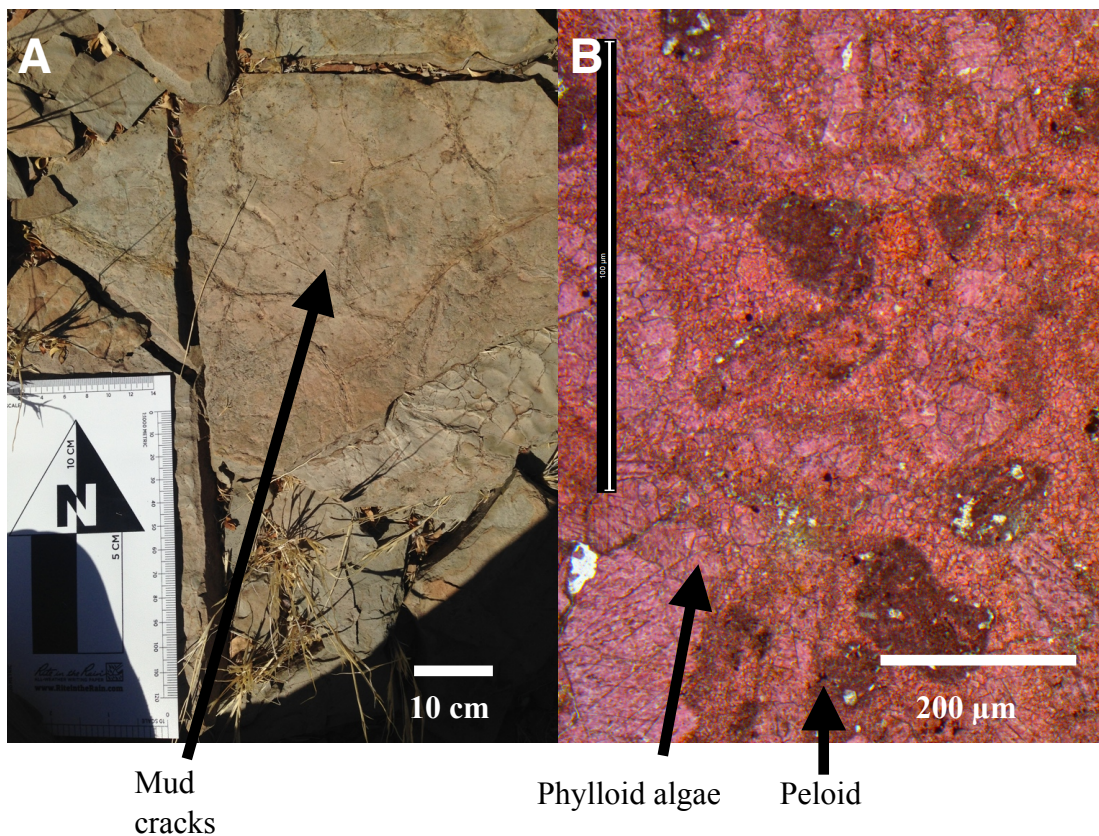


Figure 10. Photographs of the phylloid algal peloidal grainstone lithofacies. A) Outcrop photograph of top of bed displaying mud cracks B) Thin section photomicrograph.

foram peloidal grainstone facies. The normal marine fossils, such as the phylloid algae and echinoderms, indicate that the current energy was also bringing in grains, unlike the foram peloidal grainstone lithofacies, which only brings in grains from the intertidal facies association. Finally the thinness of the bed indicates that this lithofacies was deposited with little accommodation space, which suggests an environment that is close to the paleoshoreline.

2.1.4 Carbonate Subtidal Depositional Facies Association

This lithofacies association is composed of echinoderm, bivalve, brachiopod packstone, echinoderm, phylloid algae, bivalve packstone, and *Tubiphytes* red algal packstone. Subtidal deposits form basinward of the paleoshoreline both above and below fair-weather wave base. Additionally these facies are rarely sub-aerially exposed unless there is a significant neap tide or change in sea-level related to major eustatic events. Higher energy environments occur in the shallower locations and are concentrated around fair-weather wave base. Consequently, environments that are more basinward from fair- weather wave base experience progressively less wave and tidal influences as the depositional profile deepens into the basin.

Echinoderm, Phylloid Algal, Bivalve Packstone Lithofacies

The echinoderm, phylloid algal, bivalve packstone lithofacies was only found in the Doña Ana Mountains mostly in the middle of the measured section. The beds range in thickness from 30 cm to approximately 5 meters, but most beds average around 2 meters. The beds are dark gray on outcrop and are typically capped by burrows with iron staining or a large fossils concentrated

at the top. Fresh faces are a slightly lighter gray and will occasionally have a fetid odor when broken open.

Grains are dominantly made up of phylloid algae and bivalve fossils with lesser amounts of echinoderm and brachiopod fragments, and peloids. The matrix is dominantly made up of carbonate mud which has been locally silicified (Fig. 12).

Depositional Environment Interpretations

The higher carbonate mud content in this lithofacies suggests that these sediments were deposited basinward of the grainstones, in regions of lower wave and current energy. Wilson and Jordan (1983) also suggest that finer-grained sediments are deposited on lower parts of a carbonate shelf where micrite mud can accumulate. Stoklosa et al. (1998) interprets similar

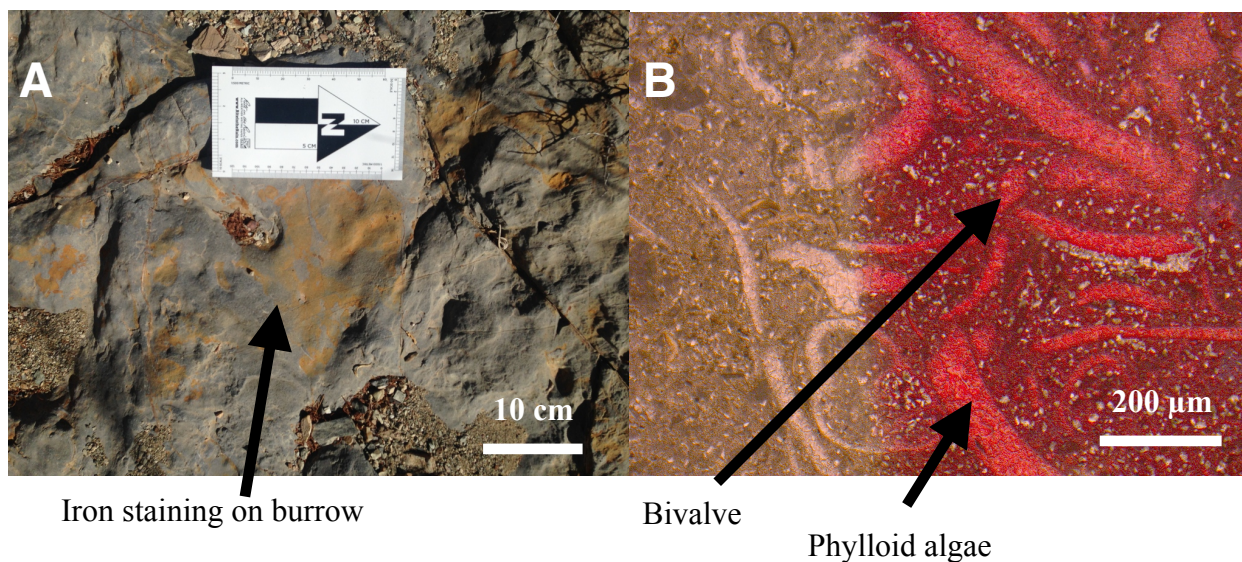


Figure 11. Photograph of the echinoderm, phylloid algal, bivalve packstone lithofacies. A) Photograph of outcrop with visible burrowing with iron staining B) Photomicrograph showing phylloid algae and bivalves

packstones from the Hueco Mountains as deposition on the shelf below wave base based on high-faunal diversity and increased mud content. However, deposition was still considered to occur in fairly shallow water with low turbidity based on the presence of benthic photosynthetic algae and filter feeders such as bryozoans.

Echinoderm, Bivalve, Brachiopod Packstone Lithofacies

Echinoderm, bivalve, brachiopod packstone is commonly found in the Robledo Mountains and rarely in the Doña Ana Mountains. Beds of this facies are common and thick at the base of the Robledos sections, gradually becoming less common and thinner higher up in the section. In outcrop this lithofacies is thin to thickly bedded ranging from 40 cm to approximately 5 m. Bedding is undulose, light gray in color on weathered faces and light gray on fresh faces. Macroscopic fossils such as abraided brachiopods and gastropods are visible on outcrop and in hand samples.

In thin section this lithofacies can be identified by a high diversity of fauna. Skeletal grains are predominantly brachiopods, bivalves, and echinoderm fragments, and lesser amounts of bryozoans, phylloid algae, and forams. The matrix of this facies is dominantly made up of carbonate mud with equant blocky fine calcite crystals filling voids (Fig. 13). The carbonate mud has also been locally silicified.

Depositional Environment Interpretations

The echinoderm, bivalve, brachiopod packstone facies is interpreted as deposited in deeper water than the echinoderm, phylloid algal, bivalve packstone facies based on the lack of photosynthetic phylloid algae. The higher carbonate mud content and lack of skeletal grain size

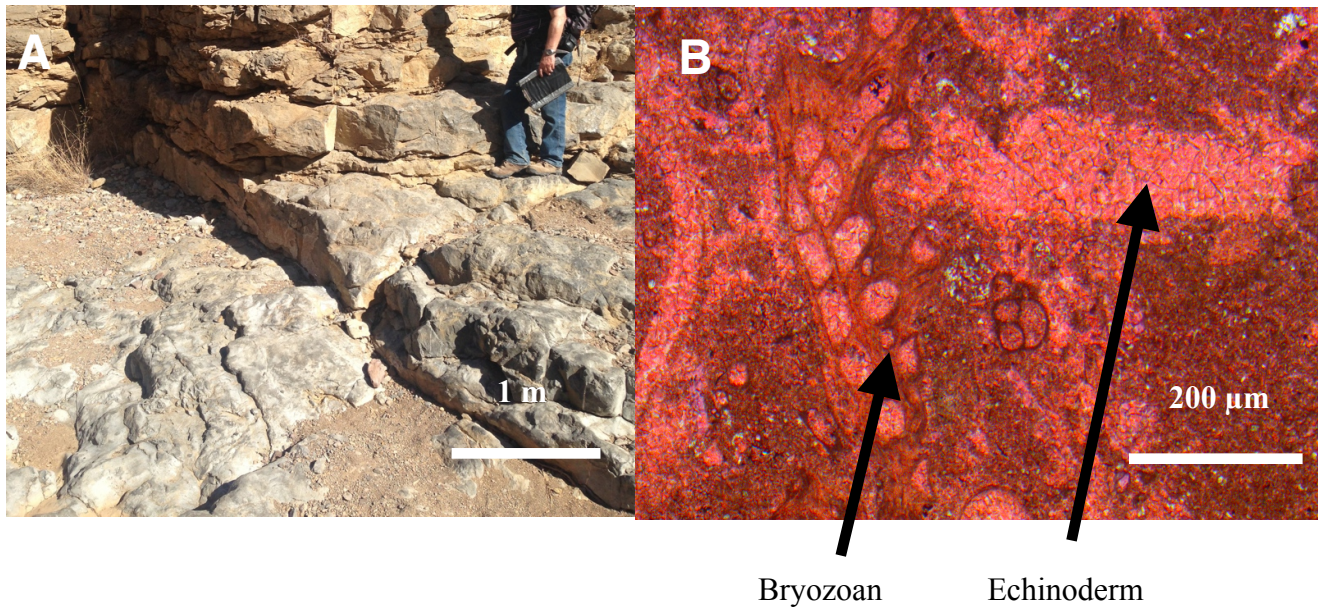


Figure 12. Photographs of echinoderm bivalve brachiopod packstone lithofacies A) Outcrop photograph of thick undulose bedding, B) Photomicrograph showing diverse, normal marine fauna, stained for calcite

sorting suggests that these sediments were deposited basinward of the grainstones, in regions of lower wave and current energy. Wilson and Jordan (1983) also suggest that finer-grained sediments are deposited on lower parts of a carbonate shelf where micrite mud can accumulate. Stoklosa et al. (1998) interprets similar packstones from the Hueco Mountains as deposition on the outer shelf below wave base based on high-faunal diversity and increased mud content. The lack of phylloid algae in this lithofacies suggests that this environment experienced less sunlight and was thus deeper or in more turbid water.

Tubiphytes Red Algal Packstone Lithofacies

The *Tubiphytes*-red algal packstone is only found in the Doña Ana Mountains section and only in one bed. The bed is 30 cm thick with irregular wavy bedding, and is capped by brown chert nodules. The most common feature is the visible red algae, *Archaeolithoporella* (Wahlman, personal correspondence) and chert nodules that formed on the top of the bed., *Tubiphytes*, also known as *Shamovella* (Riding, 1993), commonly encrusts red algae blades and occasionally fenestrate bryozoans (Fig. 14). Similar to other packstone lithofacies, dense micrite mud forms the matrix. Calcite cement is much less common. Chert nodules are still common and have formed on the top of the only bed to be found in the gastropod interval of the Hueco Limestone. The carbonate mud has also been locally silicified.

Depositional Environment Interpretations

The combination of laminar red algae with *Tubiphytes* suggest

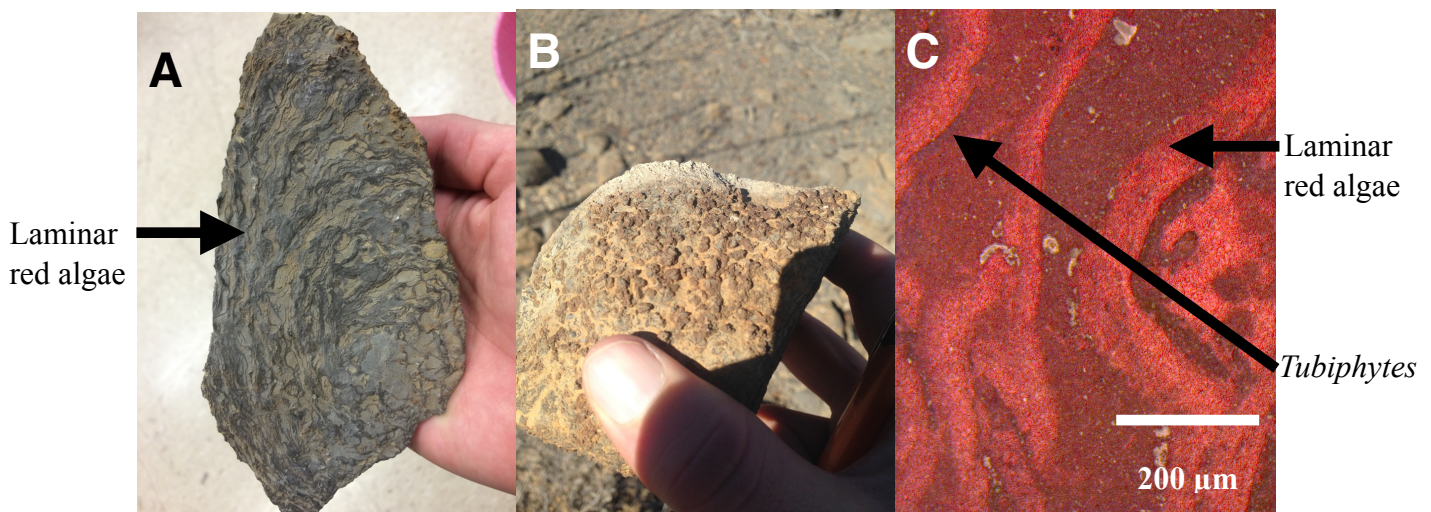


Figure 13. Photographs of the Tubiphytes red algal lithofacies. A) Photograph of hand sample showing the concentric wavy laminae of red algae B) Photograph of hand sample with brown chert nodules on top of bed C) Photomicrograph of inter-laminated red algae on Tubiphytes, stained red for calcite

deposition on deeper parts of the Robledo Shelf. The high mud content indicates low current energy, below fair weather wave base. In the Mississippian, *Tubiphytes*-fenestrate bryozoan buildups were found to be the primary constituents of Waulsortian mud mounds, which are considered as deeper water buildups compared to contemporaneous phylloid algal buildups (Lees et al., 1985; Lees and Miller, 1985). During the Early Permian, *Tubiphytes*-red algal buildups were the dominant type of organic buildup (Wahlman, 2002), was a binding organism common to the Late Paleozoic. This lithofacies appears to represent deeper, possibly colder water system and consequently represents the deepest subtidal carbonate lithofacies in the study area.

2.1.5 Siliciclastic Terrestrial Depositional Facies Association

Quartz Siltstone Lithofacies

Quartz siltstone is only found in the Doña Ana Mountains and is medium to thin bedded, ranging from 20 cm to 4.5 m, tan weathering and forms continuous tabular units with sharp upper and lower bedding boundaries. The grains are made up of well-sorted, well-rounded quartz with rare lithic grains that form asymmetrical ripples, with current direction pointing to the east, that gradually change to symmetrical ripples towards the tops of the beds. The base of these beds will sometimes shows evidence of burrow fill and the top shows a gradual change to symmetrical ripples or the top is erosional. Basal erosion was uncommon, only taking place in one of the three siltstone beds, incising down 0.5 m into unconsolidated marine shale. Lateral accretion sets 1 m high and covering a distance of about 5 m (Fig. 15). As previously stated, this facies is confined to the Doña Ana Mountains, no siltstone or sandstone beds were found in the Robledo Mountains in the upper interval of the middle Hueco.

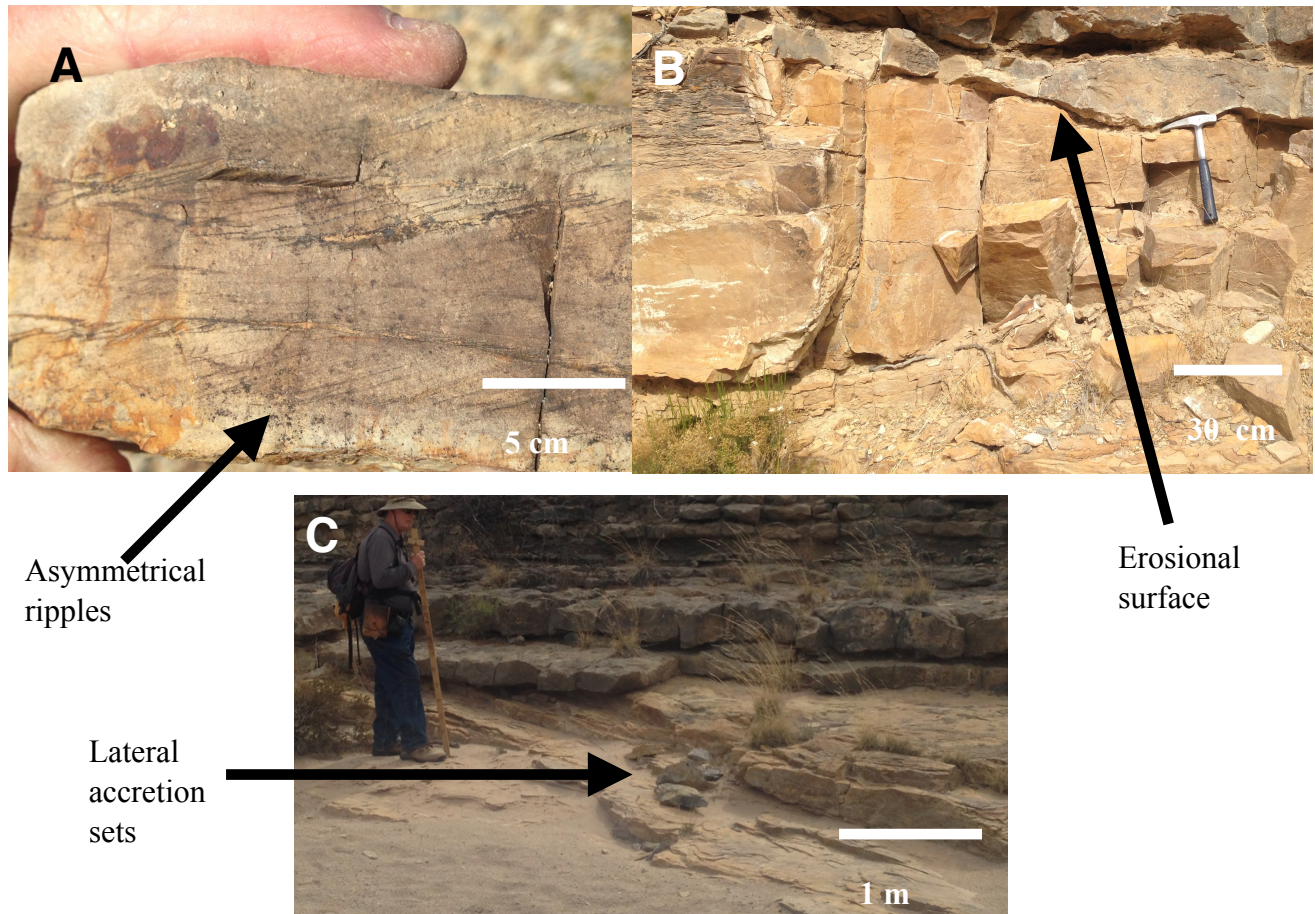


Figure 14. Photographs of quartz siltstone lithofacies. A) Photograph of hand sample showing common asymmetrical ripples B) Photograph of outcrop showing basal erosional surface of channel C) Photograph of outcrop

Depositional Environment Interpretations

The dominant sedimentary structure of this facies is the asymmetrical ripple, which is created by unidirectional current (Simons, 1960). The silt-sized grains and ripples, as well as the preservation of burrows in the shale underneath these beds indicates that current energy was low (Allen, 1971). The lateral accretion sets indicate that it was a channelized system with relatively low energy (Miall, 1985). The lack of burrows or bioturbation indicates a fluvial rather than a

marine environment. The change at the top to symmetrical ripples indicates wave action and marine influence (Allen, 1971), likely a reworking of the silt by a marine flooding event.

Vertic Calcisol Lithofacies

Only one calcisol bed was found in the Doña Ana Mountains. The soil profile was about 40 cm thick. The soil contains cracks that have been filled in with clay from another source. The soil developed on a bed of dull gray shale and contains white calcite nodules that ranged in size from 5 to 10 cm that can be found about 20 cm below the top of the bed (Fig. 16). The top 10 cm of the soil appear to be mottled with fewer cracks that developed compared to the lower layers.

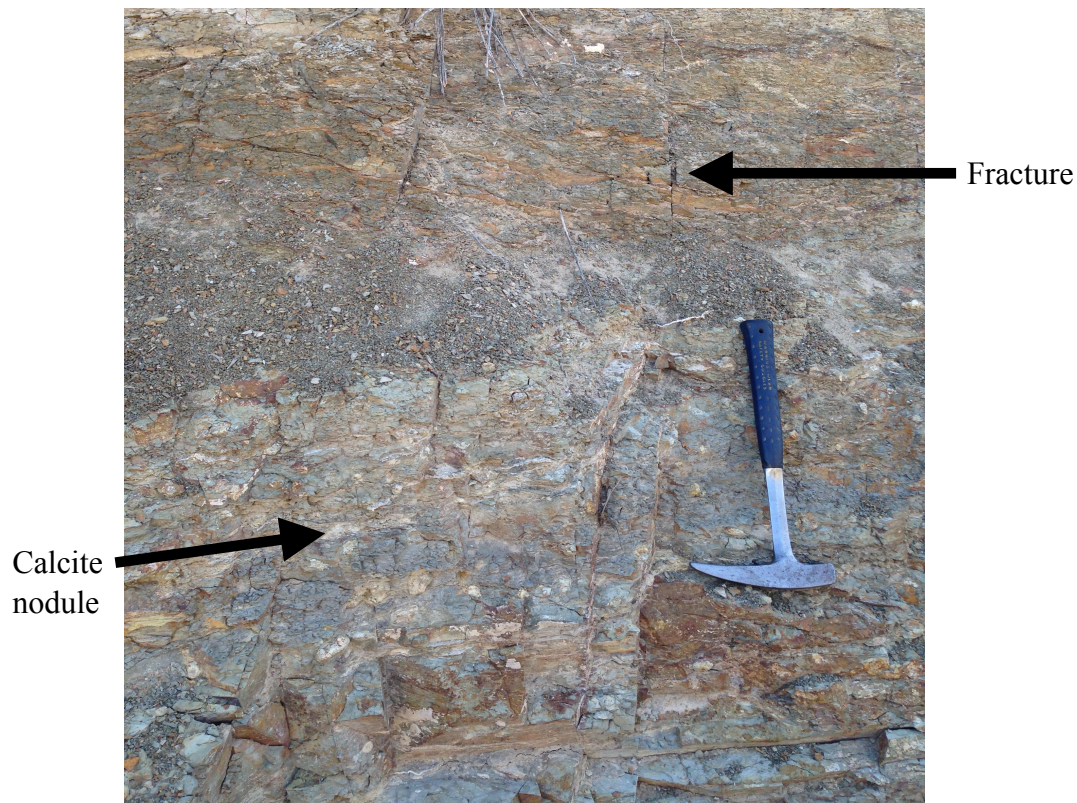


Figure 15. Outcrop photograph of vertic calcisol facies that formed within the offshore marine gray shale facies.

Depositional Environment Interpretations

The defining feature of this facies are the calcite nodules. Using the paleosol classification system from Mack et al. (1993), which defines a paleosol with a prominent calcite horizon as a calcisol, which form in semi-arid environments. Semi-arid environments are defined by average evaporation being higher than average precipitation. As documented by Gile (1966), calcite nodules that are few to common in a non-gravelly soil are part of a Stage II surface, which requires at least 5000 years to form. The cracks that developed on the soil indicate that the soil and shrink-swell clays, such as montmorillonite (Ahmad, 1983), and suggest that the climate varied between wet and dry times.

2.1.6 Siliciclastic Offshore Marine Depositional Facies Association

Gray Shale Lithofacies

Gray shale is the most common lithofacies in both the Robledo Mountains and Doña Ana Mountains. Shale beds had a wide range of thicknesses from 0.1 to 5 meters. Shale beds were often dull gray to black and fissile, slope formers and were rarely well-exposed. Well-exposed beds would sometimes contain thin laminations of silt (<1 cm) (Fig. 17). As previously stated shale beds were very common in both sections, making up about half the thickness in the Doña Ana Mountains and about a quarter of the thickness in the Robledo Mountains.



Figure 16. Photograph of outcrop of gray shale lithofacies. with Dr. Mack for scale (approximately 168 cm tall).

Depositional Environment Interpretations

The dull gray color of the shale suggests it was deposited in a reducing environment. The uniform fine-grained nature indicates deposition in a low energy environments below fair weather wave base. The laminations and lack of burrowing or root traces also indicate that this environment was low on oxygen and could not support fauna that would cause bioturbation. All of which suggest a deep offshore marine environment.

2.3 Depositional Profile Geometry

The type and distribution of the depositional facies from the gastropod interval and upper interval of the middle Hueco were used to interpret the geometry of the depositional profile of the Robledo shelf of the western margin of the Orogrande Basin. Each environment's position on the profile was defined based on the lithofacies characteristics described and interpreted depositional setting. Depositional environments were used to understand the depositional profile (Fig. 18), which summarizes the typical Waltherian facies used to construct the sequence stratigraphic framework for the gastropod interval and the upper interval of the Middle Hueco.

During carbonate deposition, the most landward environment is the supratidal flats, characterized by the fenestral dolomudstone lithofacies. These environments are cyclically flooded and sub-aerially exposed as tidal energy regularly brings seawater in. Basinward are the intertidal flats and channels, which are deposited between the diurnal marine high tide and low tide setting, but experience restriction from the open ocean, causing changes in salinity. Depositional environments in this group appear to form in a pattern that changes both perpendicular and parallel to the shoreline (Ahr, 1973; Tucker and Wright, 1990). Intertidal lagoons formed two different lithofacies depending on paleogeographic position and climate.

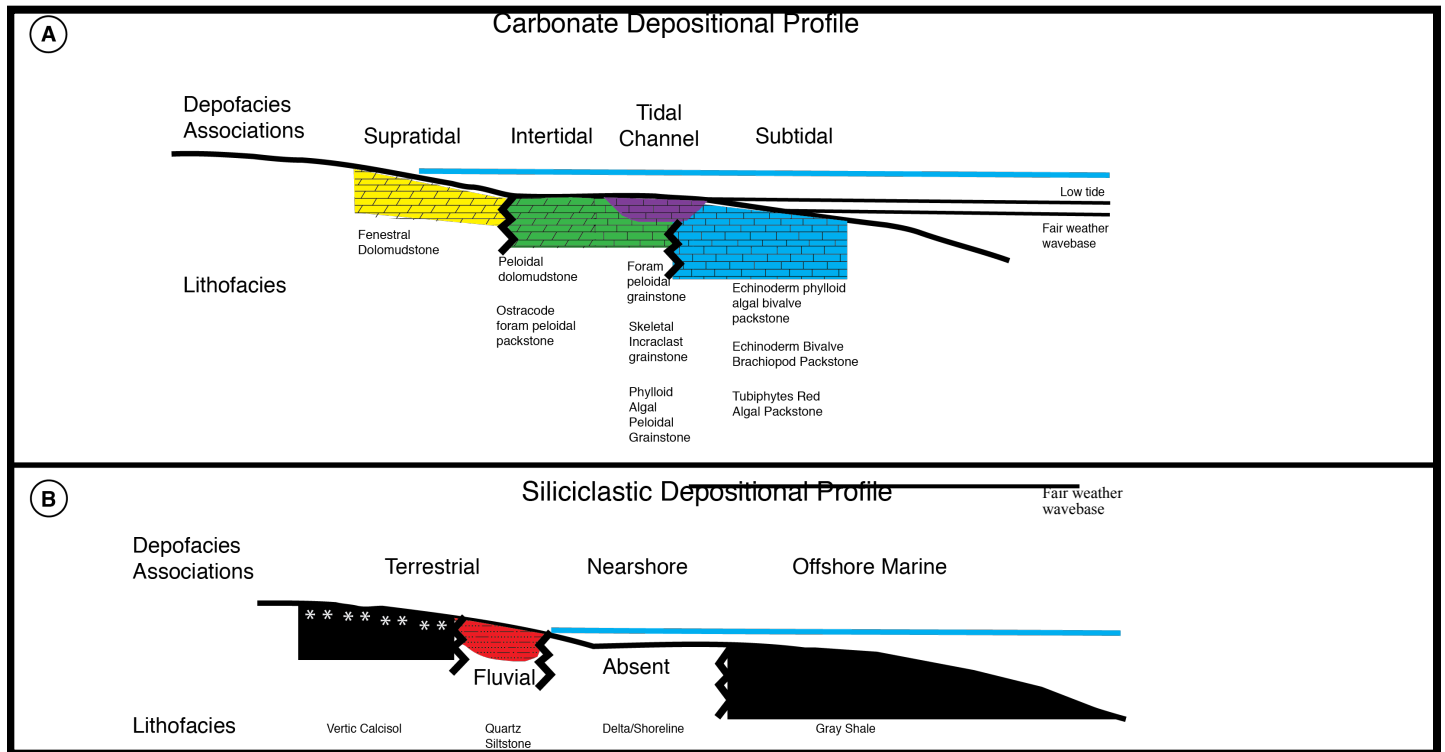


Figure 17. Schematic diagram of the terrestrial to marine depositional profile with location of depositional facies association and corresponding lithofacies. A) Carbonate depositional profile, B) Siliciclastic depositional profile.

Ostracode-foram packstone represents a restricted lagoon in which ostracodes and forams were allowed to flourish while reducing fossil diversity. Dolomudstones appear to occupy the same position on a depositional profile but represent more restricted hyper saline environment in which no invertebrate fauna could survive. Consequently, these local changes in lithofacies are representative of a delicate balance between hyper salinity and less restricted water circulation in the lagoon, rather than a significant change in sea level.

Laterally and down dip from intertidal environments are the tidal channel environments which were only periodically subaerially exposed. These are environments in which tidal energy was focused, bringing seawater from the subtidal area to the intertidal and supratidal areas. Tidal channels that formed in the high intertidal were exposed with every ebb tide while tidal channels in the low intertidal were rarely subaerially exposed.

Down dip from the tidal channels are the subtidal environments made up of fossiliferous packstones. These environments had normal marine salinities and low turbidity. Fossiliferous packstones cover the majority of the carbonate ramp and would have spanned large areas of the Robledo Shelf. Packstones formed in environments that were below fair-weather wave base and extend out to near the shelf margin, with occasional winnowing by storm waves that transported sediments landward. No subtidal facies above fair weather wave base was documented.

Basinward in deeper water water, the Tubiphytes-red algal packstones could be found. Red algae is more tolerant of deeper water, lower light, and lower temperature conditions. Thus this facies represents the deepest carbonate environment observed in the gastropod interval and upper interval of the Hueco Limestone. Finally, the most basinward lithofacies, the offshore

marine shale, which experienced low energy and a low-oxygen reducing environment, making it the deepest depositional environment in both sections.

During siliciclastic deposition, the terrestrial environments are represented by paleosols and fluvial siltstones, which experienced no marine influence. Basinward, of the terrestrial environments are the nearshore environments, where deltaic or shoreline deposits would be expected, but neither environment was documented in either section. The deepest environment is the offshore marine depofacies, represented by the gray shale lithofacies.

During the late Paleozoic, carbonate sequences formed thick aggrading and prograding packages deposited on depositional profiles ranging from low angle ramps to high relief carbonate platforms with a pronounced shelf-slope break (Vail, 1987; Posamentier and Vail, 1988). The carbonate ramp which is characterized by a shallow consistent slope from the shoreline to the basin (Ahr, 1973). The carbonate platform is characterized by a steep slope in from the basin to a reef or shoal, which absorbs most of the wave energy followed by a low energy, shallow sloping back reef area(Wilson, 1975). The western margin of the Orogrande Basin was most likely deposited in a ramp geometry, due to the lack of reef or shoal buildups seen, despite documenting carbonate depositional environments that range from the supratidal to below fair weather wave base. Similarly, during siliciclastic deposition, the shoreline environment, associated with wave action was also not documented. Without reefs or shoals to absorb wave energy this was likely not a platform, but a ramp with a geometry of restriction to protect the Robledo and Doña Ana Mountains from wind and wave energy.

Chapter 3 Depositional Sequence Stratigraphy

Carbonate sequence stratigraphy is different from siliciclastic sequence stratigraphy based on the sediment source and depositional profile geometry where carbonate deposits occur (Catuneanu, 2006). Many workers have defined how depositional profile geometry can alter the sequence stratigraphic framework for a region (Vail et al., 1977; Van Wagoner et al., 1988; Sarg, 1988). However, tectonic subsidence, eustatic sea-level change, sediment volume, and climate are the main controls on facies distribution and stratal stacking patterns in carbonate-dominated depositional environments (Vail and Todd, 1981; Sarg, 1988). This study utilized the temporal distribution of depositional environments to understand how these controls affect the sequence stratigraphic framework of the upper Middle and gastropod intervals of the Hueco Limestone. Techniques outline by Posamentier and Vail (1988), Van Wagoner et al., (1988), Sarg (1988), Catuneanu (2006) of subdividing the rock units by identifying non-Waltherian changes in depositional facies, were used to construct the sequence stratigraphic framework of this study. Stratigraphic analysis of lithofacies associations, observed on the Robledo Shelf, along the western margin of the Orogrande Basin were used as the basis to interpret the Waltherian facies progressions and sequence stratigraphic framework for this margin.

3.2 Parasequence Types

The first step in the sequence stratigraphic analysis was to identify parasequences (Fig. 19). Parasequences are shallowing upward Waltherian facies progressions bounded by marine flooding surfaces (fs). Depofacies analysis was used to define parasequences, in order to identify Waltherian and non-Waltherian facies changes. Six parasequence types are recognized (Fig. 19):

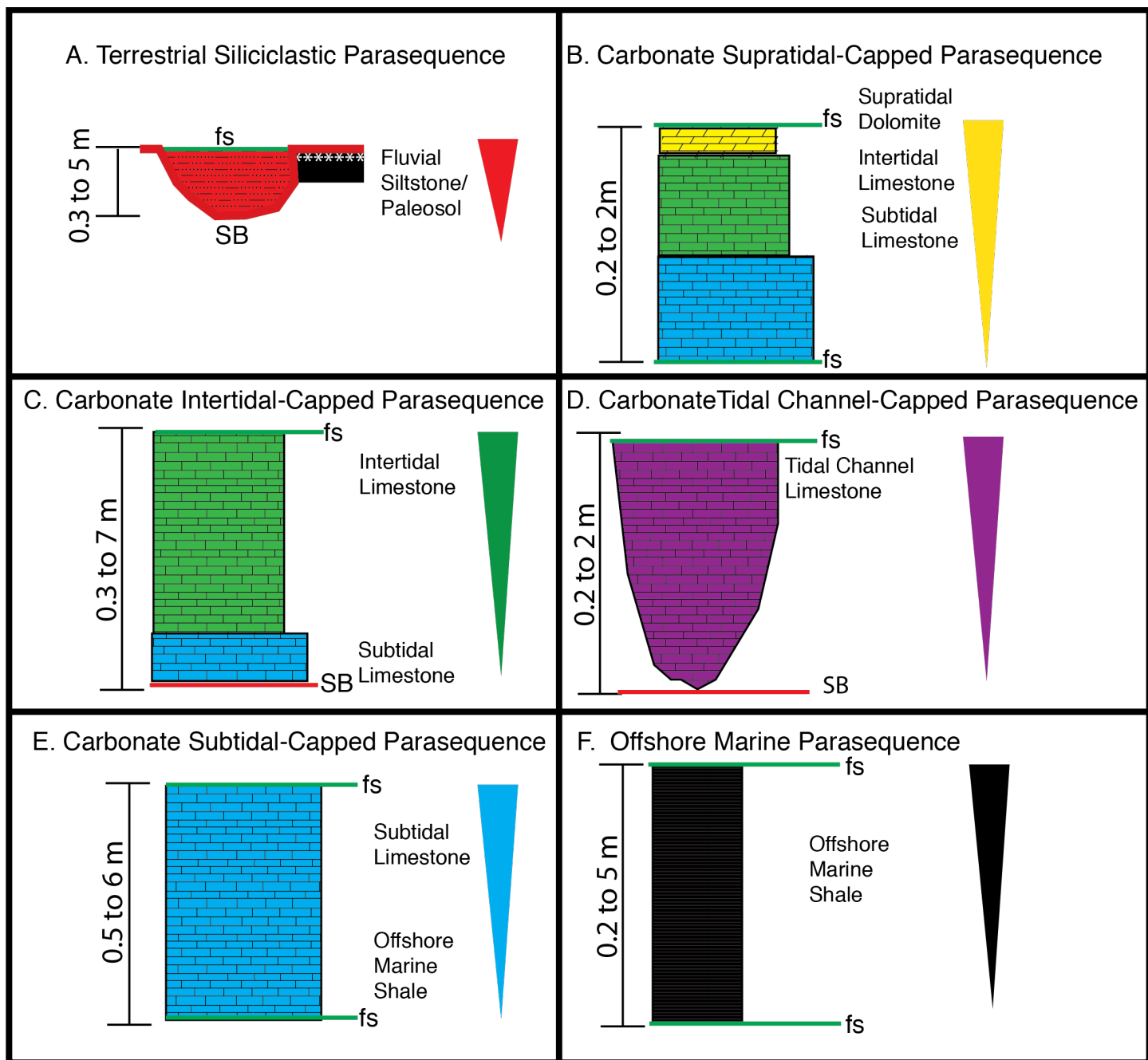


Figure 18. Examples of the six types of parasequences found in the middle and gastropod intervals of the Hueco Limestone: A) Terrestrial siliciclastic parasequence, B) Carbonate supratidal-capped parasequence, C) Carbonate intertidal-capped parasequence, D) Carbonate tidal channel-capped parasequence, E) Carbonate subtidal-capped parasequence, F) offshore marine parasequence. Green line indicates marine flooding surface.

1)

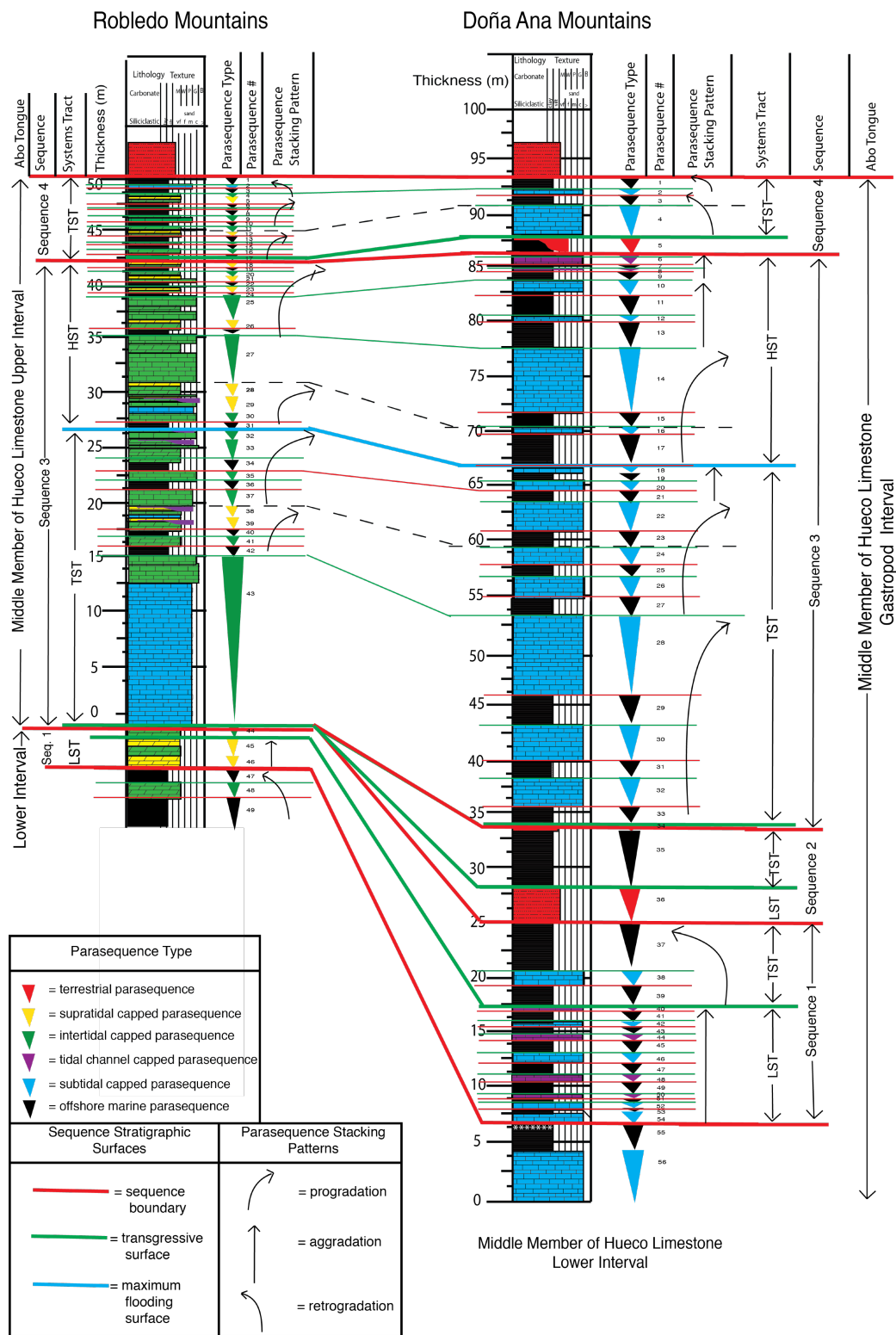


Figure 19. Measured sections with sequence stratigraphic interpretation of significant surfaces, parasequence types, and parasequence set stacking patterns.

Terrestrial siliciclastic, 2) carbonate supratidal-capped, 3) carbonate intertidal-capped, 4) carbonate tidal channel capped, 5) carbonate subtidal capped and 6) offshore marine shale. Each parasequence consists of one to five lithofacies, which reflects their formational position on the depositional profile, eustatic sea-level fluctuation, and local subsidence.

Terrestrial Siliciclastic Parasequences

Terrestrial siliciclastic parasequences are rare and only found at three levels in the gastropod interval of the Hueco Limestone in the Doña Ana Mountains (Fig. 20). They are thin, 1 to 5 meters thick. This parasequence type is made up of one of two lithofacies, fluvial quartz siltstone, and vertic calcisol. Terrestrial siliciclastic parasequences consistently occur above shale parasequences, which mark an abrupt non-Waltherian basinward facies shifts and thus represents a sequence boundaries (Van Wagoner, 1988). The terrestrial siliciclastic parasequences are consistently overlain by offshore marine shale or carbonate subtidal-capped parasequence marking a marine flooding surface at the top.

Carbonate Supratidal-Capped Parasequences

Supratidal-capped parasequences are only found in the middle member of the Hueco in the Robledo Mountains, where they are common, and are generally much thinner on average than the other parasequence types at about 0.2 to 2 meters thick. The basal bed generally consists of subtidal echinoderm, bivalve, brachiopod packstone, overlain by intertidal ostracode-foram limestone and/or restricted marine peloidal dolomudstone, and capped by fenestral dolomudstone. Supratidal parasequences are deposited above fair-weather wave base very close

to the shoreline, which had limited accommodation space, resulting in thin parasequences.

Supratidal parasequences are generally bounded by carbonate intertidal-capped parasequences or other supratidal parasequences, with rare shale parasequences. Supratidal parasequences are the shallowest parasequences found in the Robledo Mountains section.

Carbonate Intertidal-Capped Parasequences

Intertidal capped parasequences are restricted to the Robledo Mountains section. These parasequences range in thickness from 0.3 to 7 meters. The basal bed is usually made up of subtidal echinoderm, bivalve, brachiopod packstone, and capped by foram-ostracode limestone or peloidal dolomudstone. Intertidal-capped parasequences were deposited in deeper water than the carbonate supratidal-capped parasequences with greater accommodation space and greater cycle thickness. Carbonate intertidal-capped parasequences tend to be bounded by other carbonate intertidal-capped marine parasequences or supratidal parasequences and occasionally shale parasequences.

Carbonate Tidal Channel-Capped Parasequences

Carbonate tidal channel-capped parasequences are common in the Doña Ana Mountains section, where they ranged in thickness from 0.2 to 2 m. This parasequence type is usually made up of only one lithofacies, tidal channel facies, such as phylloid algal peloidal grainstone or foram peloidal grainstone. Tidal channel capped parasequences are generally bounded by subtidal capped parasequences or other tidal channel parasequences.

Carbonate Subtidal-Capped Parasequences

Carbonate subtidal-capped parasequences are only found in the Doña Ana Mountains section where they were common. Subtidal capped parasequences are 0.55 to 6 meters thick, making them the thickest parasequences in either section. This parasequence type is made up of only one lithofacies, subtidal, normal marine fossiliferous limestone. Subtidal capped parasequences are the deepest carbonate parasequences and had the greatest accommodation space, which is shown by the greatest cycle thickness. Subtidal parasequences are bounded by either other subtidal parasequences or tidal channel parasequences.

Offshore Marine Shale Parasequences

Offshore marine shale parasequences are found in both the Doña Ana and Robledo mountains sections, at four stratigraphic levels. These parasequences are 0.2 to 5 meters thick and are made up of only one lithology, gray shale. These parasequences are always capped by sequence boundaries overlain by the terrestrial siliciclastic parasequences or carbonate parasequences.

3.3 Sequences

Sixteen fourth-order sequences were identified in the Robledo Mountains and 22 fourth-order sequences were identified in the Doña Ana Mountains section. These were identified by non-Waltherian changes in sea level, from deep to shallow marine, while sea level changes to terrestrial environments were interpreted as third-order level changes.

Five third order sequence boundaries (Fig. 20) are identified in the Doña Ana Mountains section, all associated with an abrupt non-Waltherian basinward shift in facies to terrestrial fluvial or paleosol environments. These sequence boundaries divide the Doña Ana Mountains gastropod interval section up into four third-order sequences and 22 fourth-order. The uppermost sequence boundary between the gastropod interval and the Abo Tongue. Four third-order sequence boundaries are identified in the Robledo Mountains section, defining 3 third-order sequences and 16 fourth-order sequences. Correlation between the Doña Ana and Robledo mountains sections was started using the sequence boundary associated with the base of the Abo Tongue, and moving progressively down section, correlating sequence boundaries. Further detailed correlation was done using matching parasequence stacking patterns. Three styles of stacking patterns are identified: 1) retrogradational, which were characterized by parasequences capped by deeper facies upward, 2) aggradational, which were characterized by parasequences staying the same depth upward, and 3) progradational, which were characterized by parasequences capped by shallower sequences upwards.

Sequence 2 in the Robledo Mountains was characterized by non-deposition. This is identified by the Doña Ana Mountains section in Sequence 2 to be dominated by siliciclastics and fluvial environments. The Robledo Mountains section contained shallower depofacies, and because there are no terrestrial environments in the Middle Member of the Hueco Limestone (Seager, 2008, Mack et al., 2013) it was interpreted as non-deposition.

Sequence 1

The base of Sequence 1 in the Doña Ana Mountains is several fourth-order sequences above the base of the gastropod interval, whereas in the Robledo Mountains section it is several parasequences below the top of the lower interval of the Middle Member of the Hueco Limestone. In the Doña Ana Mountains it is bounded on the base by the third-order sequence boundary associated with the vertic calcisol facies superimposed on the offshore marine shale facies. In the Robledo Mountains, the sequence boundary is below below supratidal fenestral dolomudstone that sits directly on offshore marine shale. The level of subaerial exposure of offshore marine shale is similar in both sections. Sequence 1 is the second thickest sequence in the Doña Ana Mountains (at 19 m) and the third thickest in the Robledo Mountains.

Sequence 1 contains the low stand (LST) and transgressive (TST) systems tract in the Doña Ana Mountains is made up of several thin carbonate subtidal-capped and carbonate tidal channel-capped parasequences stacked aggradationally. In the Robledo Mountains the sequence is made up of two thin supratidal-capped parasequences, also stacked aggradationally. The transgressive surface was chosen at the abrupt shift from thin aggradational subtidal and tidal channel-capped parasequences to a thick retrogradational stack composed of deeper water subtidal-capped and offshore marine parasequences. The transgressive systems tract was only preserved in the Doña Ana Mountains.

Sequence 2

Sequence 2 is thin (~8 m) and present only in the Doña Ana Mountains section. Sequence 2 is interpreted as either non-deposition in the Robledo Mountains or as erosional removed at the

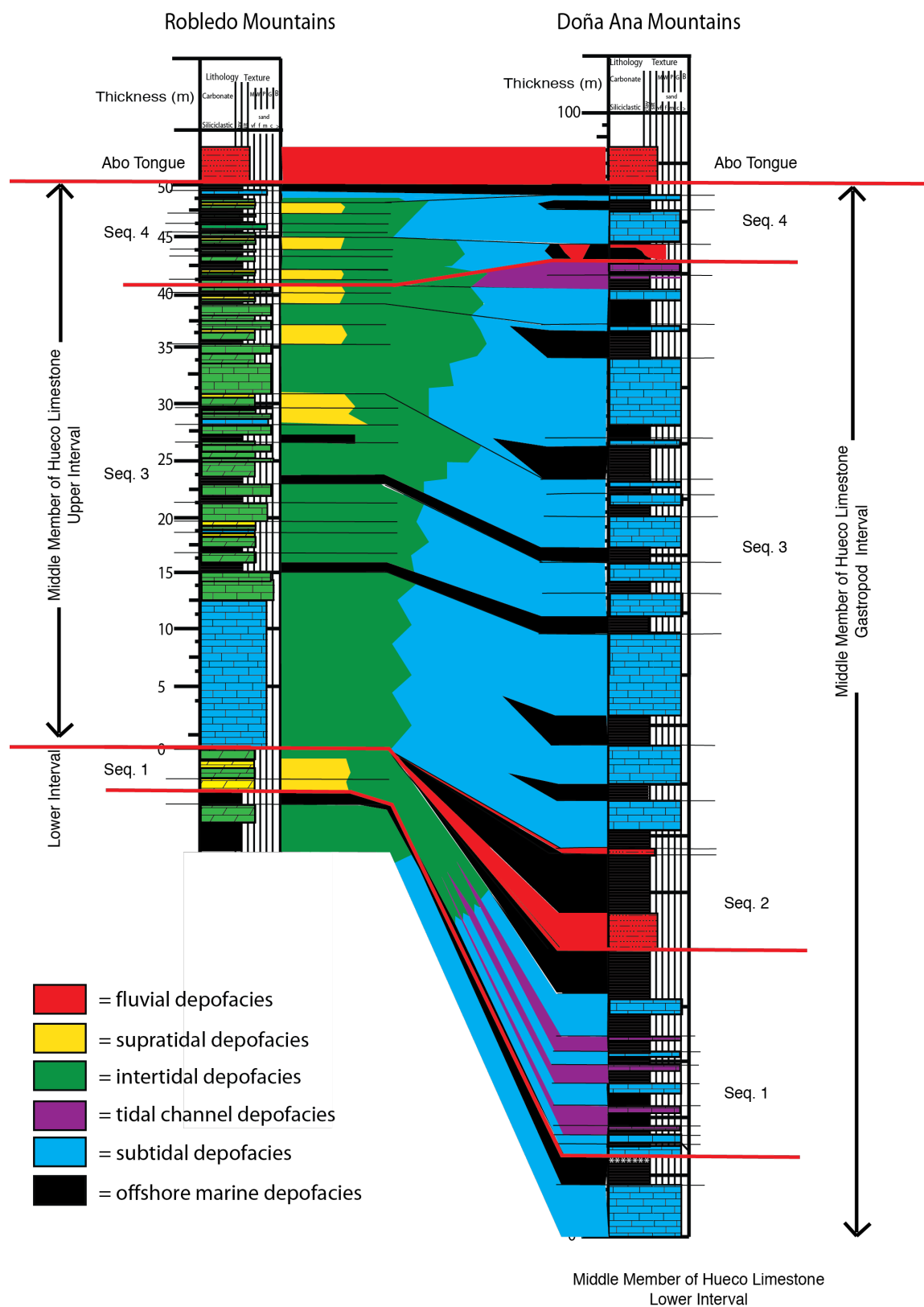


Figure 20 Measured section with interpretation of facies, correlation, systems tracts, and sequences between the Robledo and Doña Ana mountains sections..

Sequence 3 basal boundary. This sequence is the third thickest in the Doña Ana Mountains (~8 m) and lacks any carbonate lithofacies. Sequence 2 is made up of only two fourth-order sequences each containing only two lithofacies. The low stand systems tract contains the fluvial quartz siltstone. The abrupt major marine flooding surface on top of the fluvial siltstone marks the transgressive surface and the beginning of the transgressive systems tract, which comprises of a single shale parasequence.

Sequence 3

Sequence 3 is identified in both the Doña Ana and Robledo Mountains. It is the thickest third-order sequence in both sections, and also saw the deepest facies in both sections as well.

The lowstand systems tract is present only in the Doña Ana Mountains, where it is made up of only a thin bed of fluvial quartz siltstone. The upper part of the quartz siltstone was reworked in the lower shoreface during marine transgression forming symmetrical ripples and marking the transgressive surface.

The transgressive systems tract is marked by an abrupt increase in parasequence thickness from less than 1 m to greater than 5 m and a change to subtidal capped and shale parasequences from terrestrial parasequence type. In the Robledo Mountains, the base of the transgressive systems tract is made up of an unusually thick parasequence (15 m), dominated by subtidal limestone facies overlain by thinner (1-2 m) supratidal to intertidal-capped parasequences.

The maximum flooding surface is marked in the Doña Ana Mountains by the thickest bed of the deepest water facies, the offshore marine shale and a subsequent gradual change to thinner

shale beds. In the Robledo Mountains the highstand systems tract is marked by a change to lower accommodation space and a shift to a higher number of supratidal-capped parasequences.

Sequence 4

Sequence 4 is identified in both the Doña Ana and Robledo mountains sections. It was the thinnest third-order sequence in the Doña Ana Mountains (~7 m) section and the second thickest in the Robledo Mountains section (~7 m).

The lowstand systems tract is present only in the Doña Ana Mountains, where it is made up of a medium-thick bed of fluvial quartz siltstone, which had eroded down into a bed of offshore marine shale. In the Robledo Mountains section the lowstand systems tract is identified by non-deposition, which was interpreted based on the lack of terrestrial environments in that section to correlate to the Doña Ana Mountains.

The transgressive systems tract is identified in the Doña Ana Mountains section based on the erosive marine flooding surface that overlies the fluvial quartz siltstone. The rest of the transgressive systems, in the Doña Ana Mountains section is made up of two carbonate subtidal-capped parasequences. In the Robledo Mountains section, the transgressive systems tract directly overlies Sequence 3 and is identified by a change from supratidal-capped to intertidal-capped parasequences.

Chapter 4 Fischer Plot Analysis

Fischer plots of carbonate parasequences or cycles track the cumulative departure from mean cycle thickness, through a vertical sequence of contiguous upward-shallowing units (parasequences), these are used as a proxy for accommodation space available during deposition (Goldhammer et al., 1987; Fischer, 1964). A Fischer Plot is made by taking the total thickness of the section, and averaging it out to a constant subsidence rate. Starting at the base, cumulative parasequence thickness is then compared at each flooding surface to the linear subsidence rate, assuming that each parasequence covers the same amount of time. These differences are then mapped on the plot creating the eustatic sea level curve, in which trends in accommodation space can be seen. Fischer Plots can be used for correlation by matching the trends in accommodation space changes (increases and decreases) between two sections of overlapping age.

The Fischer Plot analysis done in this study established seven events marking changes in accommodation trends (Fig. 22) that could be correlated across both sections. The correlation performed using the Fischer Plot agrees closely with the correlation using sequence stratigraphic analysis and the parasequence stacking patterns. The Fischer plot shows a gradual decline in accommodation space in the Doña Ana Mountains section (cycles 1-6), a similar trend can be seen in the upper part of the Robledo Mountains section (cycles 14-1). Both sections saw a large increase in accommodation space, near the base of the sections cycle 27 in the Robledo Mountains section and cycles 18-16 in the Doña Ana Mountains section. After the rapid increase in accommodation space, each section experienced relative quiescence, with small differences in the parasequence thickness from the average. At the top of each section the parasequences became much thinner, as well as becoming dominated by shallower water facies in general, with

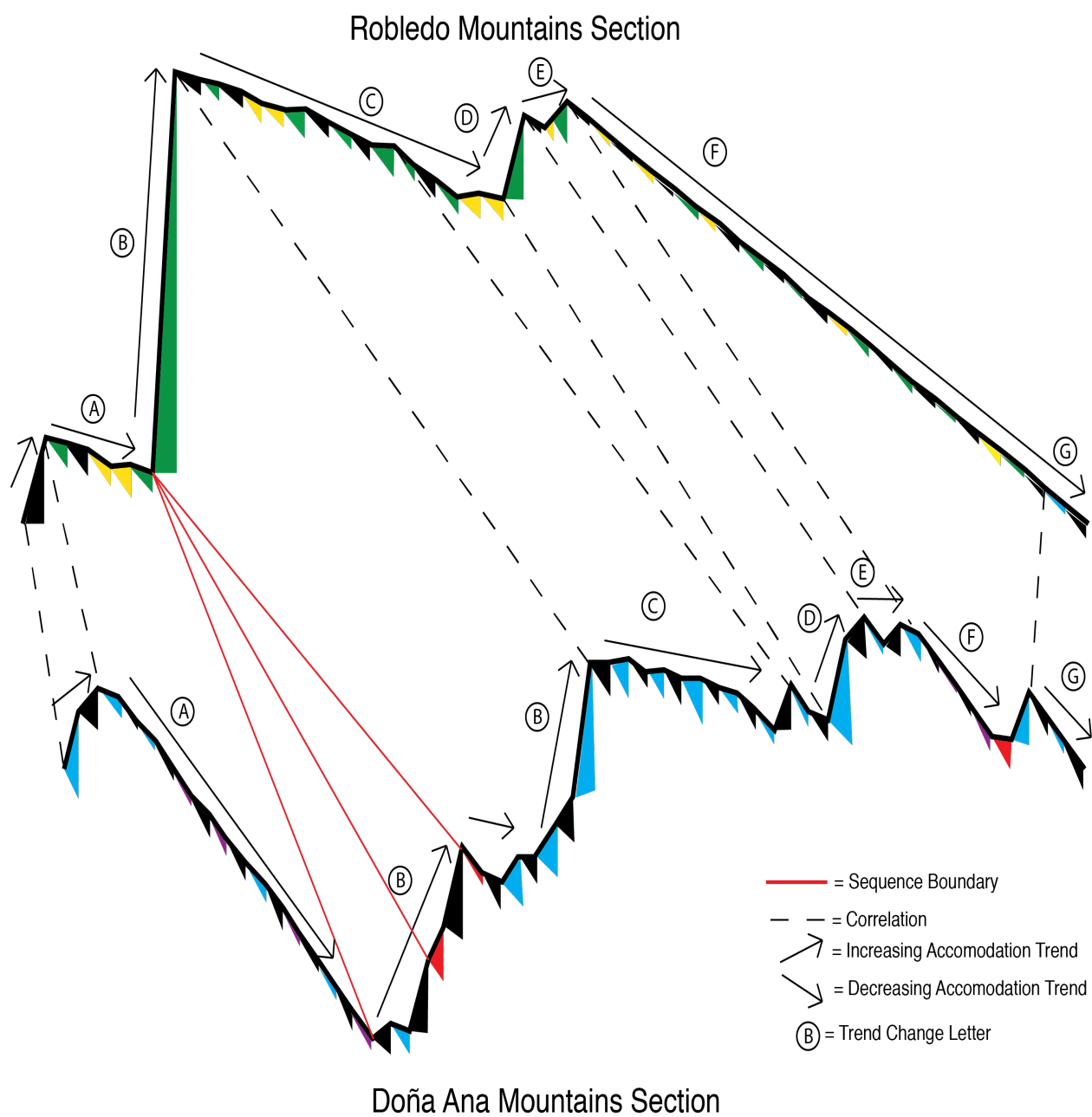


Figure 21. Fisher Accommodation Plot of the Robledo and Doña Ana mountains sections with changes in accommodation trends shown by arrows and correlation shown by the dashed lines.

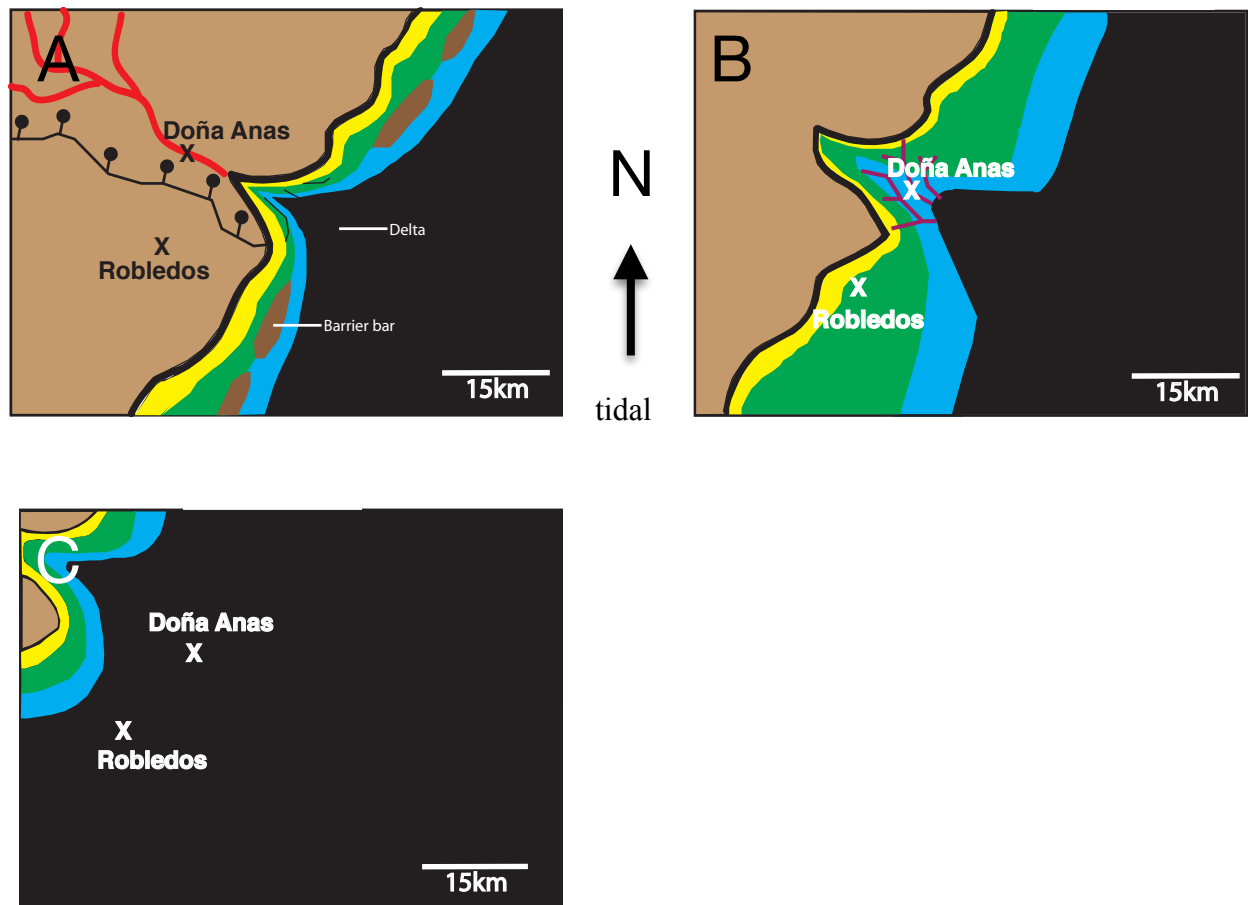


Figure 22 Paleoshoreline of the Orogrande Basin at different sealevels where red = fluvial, yellow = supratidal, green = intertidal, blue = subtidal, and black = offshore marine shale: A) lowstand systems tract, with Robledo and Doña Ana Mountains subaerially exposed, B) early transgression or late highstand, with sealevel with Robledo Mountains in an intertidal lagoon and Doña Ana Mountains in a tidal channel or subtidal, C) maximum transgression, both sections experience shale deposition.

channel and fluvial parasequences seen in the Doña Ana Mountains section and more supratidal parasequences in the Robledo Mountains section. The only spot where the Fischer Plot disagreed with the sequence stratigraphic analysis was the location of the maximum flooding surface and greatest accommodation in the Doña Ana Mountains section. The sequence stratigraphic analysis identified the maximum flooding surface as the location of the thickest shale bed (cycle 10), whereas the Fischer Plot analysis identified the location as the parasequence above that (cycle 9).

Chapter 5 Controls on Lithofacies Distribution

The distribution of Wolfcampian strata in the Orogrande Basin and Robledo Shelf was primarily influenced by glacio-eustatic sea-level changes super-imposed on a modified ramp depositional profile. Lithofacies on the Robledo Shelf represent a range of facies from fluvial to open marine depositional settings defining the Wolfcampian paleoshoreline. For these environments, relative sea-level changes had the most dramatic effect on their spatial and temporal distribution. Another control on deposition was paleobathymetry, which was a control on restriction from normal marine seawater or created a preferred conduit for lowstand fluvial channels and transgressive to highstand systems tract tidal channels (Fig. 23).

Deposition of siliciclastic and carbonate sediment did not take place at the same time in the Doña Ana and Robledo mountains section. This is apparent from the lack of siliciclastic sediment in the carbonate facies and the lack of carbonate shells or mud in the siliciclastic facies. There were also different controls on deposition for each system. The siliciclastic system is controlled by siliciclastic input into the basin and the current energy of the environment, and the carbonate system is controlled by accommodation space, current energy, light availability, and salinity.

5.1.1 Siliciclastics

Siliciclastics on the Robledo Shelf and western margin on the Orogrande Basin occur frequently, representing the sea-level maximums (gray shales) and lowstand incised valley minimums (fluvial quartz siltstones) in the gastropod intervals and upper interval of the middle member of the Hueco Limestone. The spatial distribution of low stand siliciclastics is primarily

controlled by the depositional profile geometry and topography of the region. The presence of lowstand siliciclastics in the Doña Ana section and the absence of them in the Robledo Mountains is due to either tectonically controlled topographic lows or stacked incised valleys developed during sea level lowstands. A tectonic driver between the two areas is more likely as this was a time of large offset, basin bounding fault development (refs) and the fluvial channel systems are thin, low depth/width ratios carrying fine-grained sediments. Not large integrated drainage producing deep incised valleys. Tectonic topographic relief could produce a depositional low that was longstanding/persistent from cycle to cycle and thus concentrate the fluvial sediments in the Doña Ana Mountains area. that would have funneled fluvial systems through the area, bypassing the shelf in the Robledo Mountains section area (Fig. 22A).

Siliciclastics also show up regularly above marine flooding surfaces as well in the form of offshore marine shale. Offshore marine shale was deposited during maximum transgression (Fig. 22 C) sea-level highs, at which time both the Robledo and Doña Ana mountains would be too deep for carbonate deposition. As both these areas would be affected similarly by glacio-eustatic flooding events the shale appears with the same regularity in both sections. Shale units in the Robledos sections were generally thinner than in the Doña Ana Mountains, which suggests that the shale in the Robledo Mountains experienced some erosion during sea level low stands or more gray shale was preferentially accumulated in the Doña Ana Mountains due to the greater accommodation space.

5.1.2 Carbonates

The distribution and production of carbonates on the Robledo Shelf was also controlled by sea-level changes, carbonate sediment production, as well as changes in accommodation space. These three controls temporally affected carbonate production during the Wolfcampian.

Sealevel changes largely controlled when the carbonates would be deposited. Carbonate rocks would not be deposited in times of subaerial exposure, when low stand systems tracts siliciclastics were being delivered to the shelf (Fig. 22A). Sea level changes also controlled the available accommodation space, which acted as a control on how thick the carbonate parasequences could get.

The spatial and temporal distribution of the depofacies was largely controlled by accommodation space. Supratidal and intertidal environments, the most restricted carbonate environments (Fig. 22B), would have been the most sensitive to accommodation space changes. Due to the small differences in water depth between the two environments, any change in accommodation space would cause a noticeable change in the environment. Subtidal depofacies would have experienced a smaller effect from accommodation space changes, because the subtidal depth range was much larger than the intertidal or supratidal ranges. Tidal channel environments were more immune to accommodation space changes because they were mainly lateral shifts and could be the lateral equivalent of the supratidal, intertidal, and subtidal (Fig. 22B).

Depositional trends on the Robledo Shelf were also influenced by the local paleogeography. The tectonic low mentioned above, can explain the differences between the depositional environments between the Robledo and Doña Ana sections. Depositional

environments in the Robledo Mountains are significantly shallower than their Doña Ana Mountains equivalents even accounting for eroded facies. The presence of supratidal and intertidal dolomite only in the Robledo Mountains sections and none found in the Doña Ana Mountains section indicates that the paleobathymetry was causing restriction from the open ocean in the Robledo Mountains. In the Doña Ana Mountains section, the tectonic low created more accommodation space, allowed for greater access to normal marine seawater, and created a preferred path for tidal channels through this section. This can be seen in the Doña Ana Mountains section by the greater total thickness as well as average parasequences thickness, greater number of subtidal, normal marine parasequences, and increase in tidal channel parasequences seen in the Doña Ana section compared to the Robledo section.

^{290.1}

5.2 Middle Wolfcampian Transgression

Sequence stratigraphic analysis along with Fischer accommodation plots of the gastropod interval and the ^{295.5}middle member of the Hueco Limestone revealed that relative sea-level was on average much higher at the end of gastropod interval time (Jordan, 1972) and was followed by a major sealevel drop during deposition of the Abo Tongue. This also coincides with the unconformity of the Abo Tongue directly above the gastropod and middle members of the Hueco Limestone. This progression can also be seen in the Permian eustatic sea level curve for the upper Wolfcampian developed by Ross and Ross (1987) (Fig. 24), which documents a major sea level rise and landward shift in facies in the late Lenoxian (Hueco).

The Robledo and Doña Ana mountains sections were depositionally controlled by paleobathymetry and changes in sealevel, which were steadily rising through this part of the

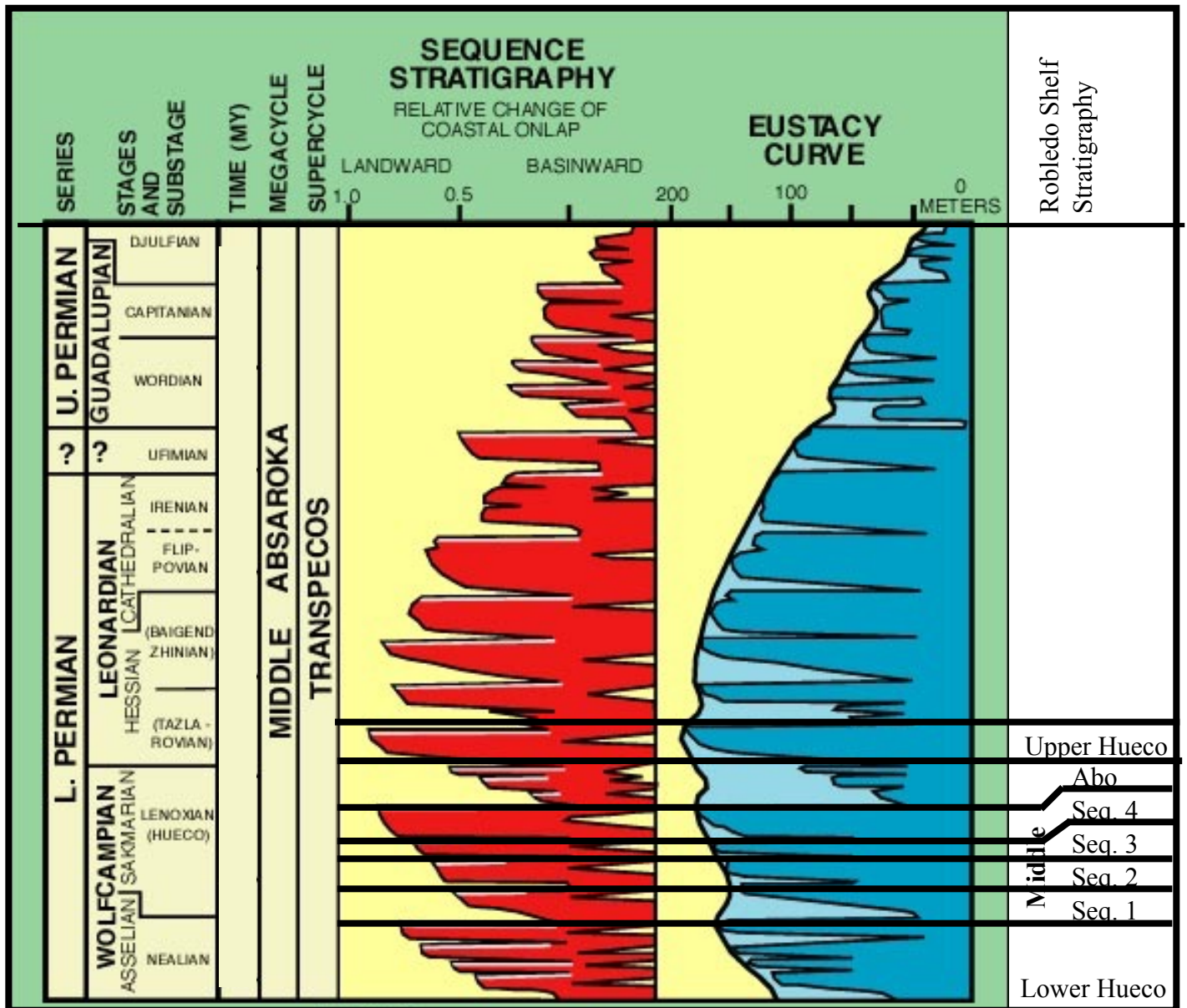


Figure 23 Permian eustatic sea level curve and relative sequence stratigraphic changes (Ross and Ross, 1987) with sea level drop associated with the transition to the Abo Tongue. Dates are from Cohen et al. (2013).

Hueco. This can be seen as a change to deeper water facies and thicker parasequences compared to the lower interval of the Middle Hueco Limestone (Mack et al., 2013).. In summary, the sequence stratigraphic analysis completed here appears to describe four progressive rises and falls in sea-level within cycles of carbonate and siliciclastic rocks deposited on the Robledo

Shelf, with an overall rise in sealevel before the large regression associated with the Abo Tongue. This is consistent with the sea level curve created by Ross and Ross (1987) establishing the global aspect of the Robledo Shelf sequences and the eustatic driver of the sequences.

On the Ross and Ross (1987) sealevel curve the Lenoxian (5.4 M.y. in time) contains four sequences. Using the classification system documented by Mitchum and Van Wagoner (1991), a sequence that lasts approximately 1 M.y. is classified as a third-order sequence.

Changes in accommodation space also have to take into account that the Orogrande Basin was subsiding at this time (Kluth and Coney, 1981), creating some accommodation space, allowing for marine sediment deposition during the sea level highstand and falling stages. This can be seen as parasequences in the Robledo Mountains becoming thinner and depofacies in the Doña Ana Mountains becoming thinner and shallower. Without subsidence deposition of the Hueco Limestone would have been limited to transgression and early highstand, before all the available accommodation space was filled.

Chapter 6 Conclusions

The gastropod interval and upper Middle member of the Hueco Limestone can be divided up into twelve distinct lithofacies including: 3 siliciclastic facies, and 9 carbonate facies. The siliciclastic lithofacies are: 1) quartz siltstone, 2) vertic calcisol, and 3) gray shale. The carbonate lithofacies are: 1) fenestral dolomudstone, 2) peloidal dolomudstone, 3) ostracode foram peloidal packstone, 4) foram peloidal grainstone, 5) skeletal intraclast grainstone, 6) phylloid algal peloidal grainstone, 7) echinoderm phylloid algal bivalve packstone, 8) echinoderm bivalve brachiopod packstone, and 9) *Tubiphytes* red algal packstone. The lithofacies were grouped into 4 depositional facies associations, which are listed below according to their relative position on a marine shoreline to basin depositional profile 1) terrestrial siliciclastic, 2) supratidal carbonate, 3) intertidal carbonate, 4) subtidal carbonate, and 5) offshore marine shale.

Sequence stratigraphic analysis of this region shows four distinctive third-order sequences within the gastropod and upper middle intervals (Fig. 21). The sequences are bounded at their bases by Type 1 sequence boundaries (Van Wagoner, 1988). Sequence 1 is characterized by subtidal and tidal channel capped parasequences in the Doña Ana Mountains and thin supratidal and intertidal capped parasequences in the Robledo Mountains. Sequence 2, is made up entirely of siliciclastics in the Doña Ana Mountains and non-deposition in the Robledo Mountains. The thickest sequence, Sequence 3, contains the lowstand, transgressive, and highstand systems tracts. Deposition is characterized by thick parasequences composed of aggradational and retrogradational intertidal capped marine and supratidal capped carbonate parasequences sets in the Robledo Mountains section and thick normal marine sequences in the Doña Ana Mountains section. Sequence 4 is characterized by thinner parasequences of restricted

and supratidal in the Robledos Mountains and normal capped marine and tidal channel capped parasequences in the Doña Ana Mountains section.

The Robledo section is overall, thinner, has shallower depositional environments and is made up of a significant amount of dolomite, and no fluvial siliciclastics. The Doña Ana section is thicker, has deeper depositional environments, contains no dolomite, and has occasional fluvial siliciclastic beds. These characteristics indicate that the Doña Ana section was deposited in a depositional low that would have had greater accommodation space for a thicker section, would have allowed for deeper depositional environments. The depositional low would have funneled fluvial systems through the area during sea level lowstand and also provided a conduit for normal marine seawater during transgression and highstand that prevented restriction for dolomite precipitation.

Correlation was done using a sequence stratigraphic analysis and Fischer Plot analysis, primarily correlating sequence stratigraphic surfaces, changes in trends in accommodation space, and changes in parasequence stacking patterns. Correlation shows that the base of the upper interval does not correlate with the base of the gastropod interval, with the gastropod interval going much lower than the upper interval. Correlation also showed that the Robledo Mountains periodically experienced non-deposition during lowstand systems tracts, while the Doña Ana Mountains section experienced fluvial deposition.

This study can help identify the distribution of unconventional reservoirs in the Permian Basin by documenting the temporal and spatial distribution of siliciclastic sediment going into the basin, which can help identify where unconventional reservoir facies, namely organic-rich siltstone were deposited in the Delaware and Midland basins.

This study has focused on illuminating these depositional and sequence stratigraphic differences observed in the upper Middle and gastropod intervals of the Hueco Limestone to compare with the older and younger strata in the Orogrande Basin and in other regions that have a similar stratigraphic architecture. It is evident that more work on the Hueco Limestone would help to understand the regional stratigraphic architecture that is more complex than once perceived. Additionally, these late Paleozoic carbonate dominated systems require very detailed outcrop, petrographic, and geochemical work to properly understand the stratigraphic architecture and depositional controls of the region.

References

- Ahr, W.M., 1973, Carbonate Ramp: alternative to Shelf Model: The American Association of Petroleum Geologists, Bulletin 57 (9), p. 1826.
- Ahmad, N., 1983. Vertisols. *Developments in Soil Science*, 11, 91-123.
- Algeo, T.J., 1992, Continental-scale wrenching of southwestern Laurussia during the Ouachita-Marathon orogeny and tectonic escape of the Llano block, *in* Lindsay, R.F. and Reed, C.L., eds., *Sequence stratigraphy applied to Permian Basin reservoirs: Outcrop analogs in the Caballo and Sacramento Mountains of New Mexico*, West Texas Geological Society, Publication no. 92-92, p. 115-131.
- Allen, G. P., 1971. Relationship between grain size parameter distribution and current patterns in the Gironde estuary (France). *Journal of Sedimentary Research*, 41(1).
- Bathurst, R.G.C., 1975. Marine diagenesis of shallow water calcium carbonate sediments. *Annual Review of Earth and Planetary Sciences*, 2, p.257.
- Blakey, R.C., 1980. Pennsylvanian and Early Permian paleogeography, southern Colorado Plateau and vicinity. *Rocky Mountain Section (SEPM)*.
- Briggs, J. C. 1974. *Marine zoogeography*: 475p; (McGraw-Hill, New York)
- Brown, L. F., and Fischer, W. L., 1977, Seismic-stratigraphic interpretation of depositional systems: examples from Brazil rift and pull-apart basins, *in* Payton, C. E., ed., *Seismic Stratigraphy-Applications to Hydrocarbon Exploration*: American Association of Petroleum Geologists Memoir 26, p. 213-248
- Catuneanu, O., 2006. *Principles of sequence stratigraphy*. Elsevier.
- Cohen K. M.; Finney S. C.; Gibbard P. L.; Fan J. X., 2013, The ICS international chronostratigraphic chart, *Episodes* 36 (3): 199–204.
- Connolly, W.M. and Stanton Jr, R.J., 1983. Sedimentation and paleoenvironments of the Morrowan strata in the Hueco Mountains, west Texas. *Geology of the Sierra Diablo and southern Hueco Mountains, west Texas*: Society of Economic Paleontologists and Mineralogists, Permian Basin Section, Guidebook, pp.36-64.
- Copeland, B. J., 1967 Environmental characteristics of hypersaline lagoons. *Publications of the Institute for Marine Science (University of Texas)* 12: 207-218.

- Cys, J.M. and Gibson, W.R., 1988, Pennsylvanian and Permian geology of the Permian Basin region, in *Sedimentary Cover – North American craton, U.S.: The geology of North America*, Vol. D-2, Decade of North American Geology, Geological Society of America, p. 277-289.
- Deffeyes, K.S., Lucia, F.J., and Weyl, P.K., 1965, Dolomitization of recent and Plio-Pleistocene sediments by marine evaporate waters on Bonaire, Netherlands Antilles, in *Dolomitization and limestone diagenesis: Society of Environmental Paleontologists and Mineralogists Special Publication 13*, p. 71-88.
- Enos, P., 1983, Shelf Environment, in Schoelle, P.A., Debout, D.G., and More C.H., eds., *Carbonate Depositional Environments: American Association of Petroleum Geologists, Memoir 33*, p. 267-295.
- Evans, G., Schmidt, V., Bush, P.R., and Nelson, H., 1969, Stratigraphy and geologic history of the sabkha, Abu Dhabi, Persian Gulf: *Sedimentology*, Vol. 12, p. 145-159.
- Ferrill, D.A., Sims, D.W., Waiting, D.J., Morris, A.P., Franklin, N.M., and Schultz, A.L., 2004, Structural framework of the Edwards Aquifer recharge zone in south-central Texas. *Geological Society of America Bulletin*, v. 116(3-4), p. 407-418.
- Fischer, A. G., 1964, The Lofer cyclothems of the Alpine Triassic: *Kansas Geological Survey Bulletin*, v. 169, p. 107–149.
- Frakes, L. A., Francis, J. E., and Syktus, J. I., 1992, *Climate modes of the Phanerozoic*: Cambridge, UK, Cambridge University Press, 274 p.
- Gartner, S., 1977. Calcareous nannofossil biostratigraphy and revised zonation of the Pleistocene. *Marine Micropaleontology*, 2, pp.1-25.
- Gile, L. H., Peterson, F. F., & Grossman, R. B., 1966. Morphological and genetic sequences of carbonate accumulation in desert soils. *Soil Science*, 101(5), 347-360.
- Graham, S.A., Dickinson, W.R., and Ingersoll, R.V., 1975, Himalayan-Bengal model for flysch dispersal in the Appalachian-Ouachita system: *Geological Society of America Bulletin*, Vol. 86, p. 273-286.
- Heckel, P.H., 1977; Origin of physphatic black shale facies in Pennsylvanian cyclothems of Mid-Continent North America: *American Association of Petroleum Geologists Bulletin*, Vol. 61, p. 1045-1068.
- Illing, L.V., Wells, A.J., and Taylor, J.C.M., 1965, Penecontemporary dolomite in the Persian Gulf, in Pray, L.C., and Murray, R.C. eds., *Dolomitization and Limestone Diagenesis: Society of Environmental Paleontologists and Mineralogists Special Publication 13*, p. 89-111.

- Jordan, C. F., 1975. Lower Permian (Wolfcampian) sedimentation in the Orogrande basin, New Mexico. In Guidebook of the Las Cruces Country: New Mexico Geol. Soc. 26th Field Conf (pp. 109-117).
- Kendall, C.G.S.C. and Skipwith, S.P.A.E., 1969. Geomorphology of a recent shallow-water carbonate province: Khor al Bazam, Trucial Coast, Southwest Persian Gulf. Geological Society of America Bulletin, 80(5), pp.865-892.
- Kessler, J. L., Soreghan, G. S., & Wacker, H. J., 2001, Equatorial aridity in western Pangea: Lower Permian loessite and dolomitic paleosols in northeastern New Mexico, USA. Journal of Sedimentary Research, 71(5), 817-832.
- King, P.B., 1934, Permian stratigraphy of trans-Pecos Texas: Geological Society of America Bulletin, Vol. 45, p. 697-798.
- King, P.B., King, R.E., and Knight, J.B., 1945, Geology of the Hueco Mountains, El Paso and Hudspeth Counties, Texas: U.S. Geological Survey Oil and Gas Investigations, Preliminary Map No. 36, 2 sheets.
- Kluth, C.F. and Coney, P.J., 1981, Plate tectonics of the Ancestral Rocky Mountains: Geology, v. 9, p. 10-15.
- Kjerfve, B., 1986. Comparative oceanography of coastal lagoons.
- Kottlowski, F. E., 1963, Paleozoic and Mesozoic strata of southwestern and south-central New Mexico: New Mexico Bureau of Mines and Mineral Resources, Bulletin 79, 100 pp.
- Kottlowski, F. E., Flower, R. H., Thompson, M. L., and Foster, R. W., 1956, Stratigraphic studies of the San Andres Mountains, New Mexico: New Mexico Bureau of Mines and Mineral Resources, Memoir 1, 132 pp.
- Kottlowski, F.E., 1960, Summary of Pennsylvanian sections in southwestern New Mexico and southeastern Arizona: New Mexico State Bureau of Mines and Mineral Resources Bulletin 66, p. 187.
- Kottlowski, F.E. and Seager, W.R., 1988, Robledo Mountains, key outcrops in south-central New Mexico: New Mexico Geological Society, 49th Field Conference Guidebook, p. 3-4.
- Kozur, H. W., and LeMone, D. V., 1995, The Shalem Colony section of the Abo and upper Hueco members of the Hueco Formation of the Robledo Mountains, Doña Ana County, New Mexico—stratigraphy and new conodont-based age determinations; *in* Lucas, S. G., and Heckert, A. B. (eds.), Early Permian footprints and facies: New Mexico Museum of Natural History and Science, Bulletin 6, pp. 39–55.

- Kues, B. S., 1995, Marine fauna of the Early Permian (Wolfcampian) Robledo Mountains member, Hueco Formation, southern Robledo Mountains, New Mexico; *in* Lucas, S. G., and Heckert, A. B. (eds.), Early Permian footprints and facies: New Mexico Museum of Natural History and Science, Bulletin 6, pp. 63–90.
- Kues, B.S. and Giles, K.A., 2004. The late Paleozoic ancestral Rocky Mountains system in New Mexico, *in* Mack, G.H. and Giles, K.A., eds., The Geology of New Mexico, A geologic History: New Mexico Geological Society, p. 95-136.
- Lawton, T. F., Giles, K. A., Mack, G. H., Singleton, D. S., and Thompson, A. D., 2002, Lower Wolfcampian conglomerate in the southern Caballo Mountains, Sierra County, New Mexico—stratigraphy, correlation, and implications for Late Pennsylvanian–Early Permian tectonics; *in*
- Laporte, L.F., 1967, Carbonate deposition near mean sea level and resultant facies mosaic, Manlius formation (Lower Devonian) of New York State: American Association of Petroleum Geologists Bulletin, Vol. 51, p. 73-101.
- Lees, A.V., Hallet, V., and Hibo, D., 1985, Facies variation in Waulsortian buildups, Part 1 – a model from Belgium: Geological Journal, Vol. 20, p. 133-158.
- Lees, A.V., and Miller, J., 1985, Facies variations in Waulsortian buildups, Part 2 – Mid-Dinantian buildups from Europe and North American: Geological Journal, Vol. 20, p. 159-180.
- Lueth, V. W., Giles, K. A., Lucas, S. G., Kues, B. S., Myers, R. G., and Ulmer-Scholle, D. (eds.), Geology of White Sands: New Mexico Geological Society, Guidebook 53, pp. 257–265.
- Lucas, S.G., Heckert, A.B., Estep, J.W., and Cook, C.W., 1998, Stratigraphy of the Lower Permian Hueco in the Robledo Mountains, Doña Ana County, New Mexico: New Mexico Museum of Natural History and Science Bulletin No. 12, p. 43-55.
- Machel, H. G. (2004). Concepts and models of dolomitization: a critical reappraisal. Geological Society, London, Special Publications, 235(1), 7-63.
- Mack, G.H., 2003, Lower Permian terrestrial paleoclimate indicators in New Mexico and their comparison to paleoclimate models, New Mexico Geological Society Guidebook, 54th Field Conference, Geology of the Zuni Plateau, p. 231-240.
- Mack, G. H., James, W. C., & Monger, H. C., 1993. Classification of paleosols. Geological Society of America Bulletin, 105(2), 129-136.
- Mack, G. H., & James, W. C., 1986. Cyclic sedimentation in the mixed siliciclastic-carbonate Abo-Hueco transitional zone (Lower Permian), southwestern New Mexico. Journal of Sedimentary Research, 56(5).

- Mack, G. H., Giles, K. A., & Durr, C. W., 2013. Sequence stratigraphy of the lower-middle Hueco transition interval (lower Permian, Wolfcampian), Robledo Mountains, New Mexico. *NEW MEXICO GEOLOGY*, 35(2).
- Mack, G. H., 2007. Sequence Stratigraphy of the lower Permian Abo member in the robledo and Doña Ana Mountains near Las Cruces, new Mexico. *New Mexico Geology*, 29, 3-12.
- Mazzullo, S.J., 1989. Lower Permian platform and basin depositional systems, northern Midland Basin, Texas.
- Miall, A.D., 1985. Architectural-element analysis: a new method of facies analysis applied to fluvial deposits.
- Miller, K. B., McCahon, T. J., & West, R. R. (1996). Lower Permian (Wolfcampian) paleosol-bearing cycles of the US Midcontinent: evidence of climatic cyclicity. *Journal of Sedimentary Research*, 66(1).
- Miller, J.A.L., Marshall, L., Heller, L.M. and Hughes, L.M., 2006. Low-level otoacoustic emissions may predict susceptibility to noise-induced hearing loss). *The Journal of the Acoustical Society of America*, 120(1), pp.280-296.
- Mitchum, R.M. and Van Wagoner, J.C., 1991. High-frequency sequences and their stacking patterns: sequence-stratigraphic evidence of high-frequency eustatic cycles. *Sedimentary Geology*, 70(2), pp.131-160.
- Moore, N. H., and D. J. Slinn., 1984 The physical hydrology of a lagoon system on the Pacific coast of Mexico. *Estuarine, Coastal and Shelf Science* 19, no. 4: 413-426.
- Morse, J. W., & Mackenzie, F. T., 1990. *Geochemistry of sedimentary carbonates*. Elsevier.
- Parrish, J. T., 1993, Climate of the supercontinent Pangea. *The Journal of Geology*, 215-233.
- Pujalte, V., Robles, S., Robador, A., Baceta, J.I. and Orue-Etxebarria, X., 1993. Shelf-to-Basin Palaeocene Palaeogeography and Depositional Sequences, Western Pyrenees, North Spain. *Sequence Stratigraphy and Facies Associations*, pp.369-395.
- Posamentier, H.W. and Vail, P.R., 1988. Eustatic control on clastic sedimentation II-sequence and systems tract models. *Sea Level Changes: An Integrated Approach*. CK Wilgus, BS Hastings, CA Ross, HW Posamentier, J. van Wagoner and CG St. C. Kendall (eds.). *Society of Economic Paleontologists and Mineralogists Special Publication*, 42, pp. 125-154.

- Pfefferkorn, H. W., 1995, We are temperate climate chauvinists: *Palaos*, v. 10, p. 389–391.
- Pray, L. C., 1961, Geology of the Sacramento Mountains escarpment, Otero County, New Mexico: New Mexico Bureau of Mines and Mineral Resources, Bulletin 35, 144 pp.
- Olszewski, T.D. and Patzkowsky, M.E., 2003. From cyclothems to sequences: the record of eustasy and climate on an icehouse epeiric platform (Pennsylvanian-Permian, North American Midcontinent). *Journal of Sedimentary Research*, 73(1), pp.15-30.
- Read, J.F. and Goldhammer, R.K., 1988. Use of Fischer plots to define third-order sea-level curves in Ordovician peritidal cyclic carbonates, Appalachians. *Geology*, 16(10), pp. 895-899.
- Riding, Robert. 1991. *Calcareous Algae and Stromatolites*, pp. 32. Springer-Verlag Press.
- Riding, R., 1993. *Shamovella obscura*: the correct name for *Tubiphytes obscurus* (Fossil). *Taxon*, pp.71-73.
- Ross, C.A., and Ross, J.R.P., 1988, Late Paleozoic transgressive-regressive deposition, in C.K. Wilgus, B.S. Hastings, C.G.St.C. Kendall, H.W. Posamentier, C.A. Ross and J.C. Van Wagoner, eds., *Sea-Level Changes: An Integrated Approach*: Society of Environmental Paleontologists and Mineralogists Special Publication 42, p. 227-247.
- Ross, C.A., and Ross, J.R.P., 1986, Paleozoic paleotectonics and sedimentation in Arizona and New Mexico, in *Paleotectonics and sedimentation in the Rocky Mountain region, United States*: American Association of Petroleum Geologists, Memoir 41, p. 653-668.
- Ross, J.R.P. and Ross, C.A., 1990, Late Paleozoic bryozoan biogeography, in McKerrow, W.S., and Scotese, C.R., eds., *Paleozoic Paleogeography and biogeography*: Geological Society of London, Memoir 12, p. 353-361.
- Sarg, J.F., 1988, Carbonate sequence stratigraphy, in C.K. Wilgus, B.S. Hastings, C.G.St.C. Kendall, H.W. Posamentier, Ross, C.A. and Van Wagoner, J.C., eds., *Sea Level Changes: An Integrated Approach*: Society of Environmental Paleontologists and Mineralogists Special Publication 42, p. 155-182.
- Seager, W. R., and Mack, G. H., 2003, Geology of the Caballo Mountains, New Mexico: New Mexico Bureau of Geology and Mineral Resources, Memoir 49, 136 pp.
- Seager, W. R., Kottowski, F. E., and Hawley, J. W., 2008, Geologic map of the Robledo Mountain and vicinity, New Mexico: New Mexico Bureau of Geology and Mineral Resources, Open-file Report 509, 12 pp.
- Seager, W.R., 1981, Geology of Organ Mountains and southern San Andres Mountains, New Mexico: New Mexico Bureau of Mines and Mineral Resources, Memoir 36, p. 97.

- Schlager, W. (1981). The paradox of drowned reefs and carbonate platforms. *Geological Society of America Bulletin*, 92(4), 197-211.
- Schlager, W., Reijmer, J. J., & Droxler, A. (1994). Highstand shedding of carbonate platforms. *Journal of Sedimentary Research*, 64(3).
- Schlager, W., 2000. Sedimentation rates and growth potential of tropical, cool water and mud mound carbonate factories. In: Insalaco, E., Skelton, P.W., Palmer, T.J. (Eds.), *Carbonate Platform Systems: Components and Interactions*. Geol Soc Lond, Spec. Publ., vol. 178, pp. 217–227.
- Schlager, W., 2003. Benthic carbonate factories of the Phanerozoic. *International Journal of Earth Sciences (Geol Rundsch)* 92, 445–464.
- Schlager, W., 2005, *Carbonate sedimentology and sequence stratigraphy*. SEPM, Tulsa, Oklahoma, 200 pp.
- Shinn, E.A., Ginsburg, R.N., and Lloyd, R.M, 1965, Recent supratidal dolomite from Andros Island, Bahamas, in Pray, L.C. and Murray, R.C., eds., *Dolomitization and Limestone Diagenesis: Society of Environmental Paleontologists and Mineralogists, Special Publication 13*, p. 112-123.
- Simons, D. B., 1960. Sedimentary structures generated by flow in alluvial channels.
- Sloss, L.L., 1963, Sequences in the cratonic interior of North America: *Geological Society of America Bulletin*, Vol. 74, p. 93-114.
- Soreghan, G.S. and Giles, K.A., 1999a, Amplitudes of Late Pennsylvanian glacioeustasy: *Geology*, v.27, p. 25-258.
- Stoklosa, M.L., Simo, J.A., and Wahlman, G.P., 1998, Facies description and evolution of a Wolfcampian (early Permian) shelf margin: Hueco Mountains, west Texas: *New Mexico Geological Society Guidebook, 49th Field Conference, Las Cruces County II*. p. 177-186.
- Tucker, M.E., Wright, V.P., 1990, *Carbonate Sedimentology* Blackwell Scientific, Oxford , p. 482
- Van Wagoner, J. C., Posamentier, H.W., Mitchum R. M., Vail, P.R., Sar, J.F., Loutit, T.S., and Hardenbol, J., 1988 An overview of the fundamentals of sequence stratigraphy and key definitions; *in* Wilgus, C.K., Hastings, B.S., Kendall, C.G., Posamentier, H.W., ross, C.A., and Van Wagoner, J.C. (eds.), *Sea-level changes —an intergrated approach: Society of Economic Paleontologists and Mineralogists, Special Publication 42*, pp. 39-45
- Vail, P.R., 1987. Seismic stratigraphy interpretation using sequence stratigraphy: Part 1: Seismic stratigraphy interpretation procedure.

- Vail, P.R. and Todd, R.G., 1981, Northern North Sea Jurassic unconformities, chronostratigraphy and sea-level changes from seismic stratigraphy, *in* Illing, L.V. and Hobson, G.D., eds., Petroleum Geology of the Continental Shelf of North-West Europe, Heyden and Son, London, p. 216-235.
- Wanless, H.R. and Cannon, J.R., 1966, Late Paleozoic Glaciation, *Earth-Science Review*, Vol. 1, no. 4, p. 247-286.
- Wahlman, G. P., and King, W. E., 2002, Latest Pennsylvanian and earliest Permian fusulinid biostratigraphy, Robledo Mountains and adjacent ranges, south-central New Mexico: New Mexico Bureau of Geology and Mineral Resources, Circular 208, 26 pp.
- Wahlman, Gregory P., and Tasker, Douglas, R., 2014 "Lower Permian (Wolfcampian) carbonate shelf-margin and slope facies, Central Basin platform and Hueco Mountains, Permian Basin, west Texas, USA." Deposits, architecture and controls of carbonate margin, slope, and basinal settings: SEPM Special Publication 105.
- Ward, R.F., Kendall, C.G.S.C. and Harris, P.M., 1986. Upper Permian (Guadalupian) facies and their association with hydrocarbons--Permian basin, west Texas and New Mexico. *AAPG Bulletin*, 70(3), pp.239-262.
- Wells, A., 1962, Primary dolomitization in Persian Gulf, *Nature*, Vol. 194, no. 4825, p. 274-275.
- Williams, T. E., 1963, Fusulinidae of the Hueco Group (Lower Permian), Hueco Mountains, Texas: Peabody Museum of Natural History, Yale Univ., Bull. 18, 123 p.
- Wilson, J.L. and Jordan, C.F., 1988, Late Paleozoic-Early Mesozoic rifting in southern New Mexico and northern Mexico: Controls on subsequent platform development, *in* Robichaud, S.R. and Gallick, C.M., eds., Basin to Shelf Facies Transition of the Wolfcampian Stratigraphy of the Orogrande Basin: Society of Environmental Paleontologists and Mineralogists, Permian Basin Section, Publication 88-28, p. 79-88.
- Wilson, J. L., and Wilson, J. L. 1975. Carbonate facies in geologic history (Vol. 471). New York: Springer-Verlag.
- Ziegler, A. M., Raymond A., Gierlowski T.C., Horrell M. A., Rowley, D. B., and Lottes, A.L., 1987, Coal, climate, and terrestrial productivity—Thre present and Early Cretaceous compared, *in* Scott, A. C., ed., Coal and coal-bearing strata—Recent advances: Geological Society of London Special Publication 32, p.25-49.

Vita

Matthew Harder was born in College Station, Texas and raised in Santa Teresa, New Mexico. Second of two children of Steve and Vicki Harder. He graduated from Santa Teresa High School in 2009 and enrolled in New Mexico State University. Matthew first majored in Civil Engineering. In 2010 he was a member of the Concrete Canoe team and was placed 11th in the nation. Matthew qualified for the Dean's List in 2011. In 2011 Matthew changed his major to Geology, where he became part of the beginning of the newly started Geology Club. After graduating in 2013. Throughout his undergraduate career Matthew did community service including Earth Day, Aggie Recycling, the Whole Enchilada, and Las Cruces MoveIt. He enrolled at the University of Texas at El Paso in 2013 to pursue a Masters of Science in geological sciences. While a graduate student he received the Chevron Earth Science Scholarship and worked as a teaching assistant for numerous classes. He participated in Imperial Barrel Award Competition as part of the UTEP 2014 team. Matthew regularly participated in volunteer work in his graduate studies helping with Earth Science Day. He also interned at Whiting Petroleum in Midland, Texas.

Contact Information: mharder42@gmail.com

This thesis/dissertation was typed by Matthew Harder.